ENGINEERING RESEARCH INSTITUTE
UNIVERSITY OF MICHIGAN
ANN ARBOR

FINAL REPORT

ON

INFRA-RED STUDIES OF CRYSTALS

(Period: 15 May 1951 to 15 May 1954)

BY

G. B. B. M. SUTHERLAND
Principal Investigator

and

C. Y. PAN LIANG

Project 1957

SIGNAL CORPS, DEPARTMENT OF THE ARMY
CONTRACT DA 36-039 sc-5581
SC PROJECT 152B-0, DA PROJECT 3-99-15-022
SQUIER SIGNAL LABORATORY, FORT MONMOUTH, N. J.

October 1954

TABLE OF CONTENTS

FINAL REPORT

ON

INFRARED STUDIES OF CRYSTALS

I. PURPOSE OF THE INVESTIGATION

The general purpose of this investigation was to use infrared analysis as a means of exploring the structure of certain crystals. In particular it was originally hoped that light could be thrown on: (a) the nature of the changes in structure which accompany the changes in the ferro-electric properties of barium titanate and possibly throw further light on the cause of the ferroelectric effect; (b) the nature of the structural differences between Type I and Type II diamonds; (c) the nature of the differences between various micas in so far as these are due to the positions of the hydrogen atoms.

As the work progressed, it seemed advisable (before tackling (c) in detail) that a simpler crystal containing OH ions should first be investigated. For this reason, a separate research was made on the infrared spectrum of brucite ($Mg(OH)_2$). In fact it turned out that the spectrum of brucite proved much harder to interpret than those of certain micas. Nevertheless, the results obtained on brucite are of considerable interest in the general field of infrared analysis of crystal structure, since these indicate that the positions of the hydrogen atoms deduced from X-ray analysis may be wrong. Alternatively, a new effect has been found in the infrared spectra of crystals which cannot be accounted for on current

theories.

II. ABSTRACT

This report gives an overall survey of research carried out between 15 May 1951 and 15 May 1954 at the University of Michigan on the infrared spectra of various crystals. There were four separate investigations which ran concurrently, the emphasis on each varying from time to time, depending on the supply of suitable personnel and other local circumstances.

The first investigation was on Barium Titanate and associated with it, some work was done on other titanates and on titanium dioxide.

The second investigation was on Diamond; associated with this were investigations on Silicon and Germanium, especially on the theoretical side.

The third investigation was on Brucite (i.e. magnesium hydroxide).

The fourth investigation was on Micas, especially muscovite, biotite and phlogopite.

This report will deal with the investigations in the above order instead of following the chronological order, although the latter corresponds to the former in a general way. Since a good deal of the detail of this work has already been reported either in quarterly or technical reports or in publications, we shall not repeat more of the detail than is considered necessary. Instead, references will

be given to earlier accounts of details and here the general results and conclusions will be emphasised. However, important details which have not been reported earlier will be given in the appropriate place.

III. PUBLICATIONS AND REPORTS

Publications

"The Infrared Spectrum of Brucite" by R. T. Mara and G.B.B.M. Sutherland, J. Opt. Soc. Amer. 43, 1100 (1953).

"The Rule of Mutual Exclusion" by T. Venkatarayudu, J. Chem. Phys. 22, 1269 (1954).

"The Infrared Spectrum of Barium Titanate" by R. T. Mara, G.B.B.M. Sutherland and H. V. Tyrell, submitted to the Physical Review, September, 1954 and will appear in November, 1954.

"The Problem of the Two Types of Diamond" by G.B.B.M. Sutherland, D. E. Blackwell, and W. G. Simeral, submitted to "Nature" September 1954 and accepted for early publication.

Talks

"Interpretation of the Infrared Spectrum of Diamond" by
W. G. Simeral and G.BB.M. Sutherland
Ohio State Symposium in Molecular Spectra at
Columbus, Ohio, June 15, 1953.

"The Location of the Hydrogen Atoms in Muscovite and Biotite"
by C. Y. Pan Liang and G.B.B.M. Sutherland
Ohio State Symposium on Molecular Spectra at
Columbus, Ohio, June 17, 1954.

"Relation between X-ray Results and the Infrared Spectra of Large Molecules" by G.B.B.M. Sutherland

Gordon Conference on Infrared Spectra at Meriden, N. H., August 5, 1954.

IV. FACTUAL DATA

IV. A. Barium Titanate

The general situation reached on barium titanate by 15th May 1954 is given in the following inset paragraphs which are a copy of a letter recently submitted for publication to the "Physics Review."

The Infrared Spectrum of Barium Titanate

The infrared absorption of barium titanate ($BaTiO_3$) has been studied between 2μ and 33μ. The spectrum obtained (Fig. A) consists of two broad bands, one centered near 550 cm^{-1}, the other starting near 450 cm^{-1} and reaching a maximum beyond 300 cm^{-1}. The low transmission in the high frequency end of the spectrum is due to scattering since the barium titanate was examined as a fine powder deposited on a KBr (or NaCl) plate from a suspension in isopropyl alcohol.

Several specimens of barium titanate were examined. The majority showed additional bands at 6.95, 9.45, and 11.65μ, which were proved to be due to carbonate ion impurities. Other impurity bands were noted at 7.1, 10.3, 11.05,

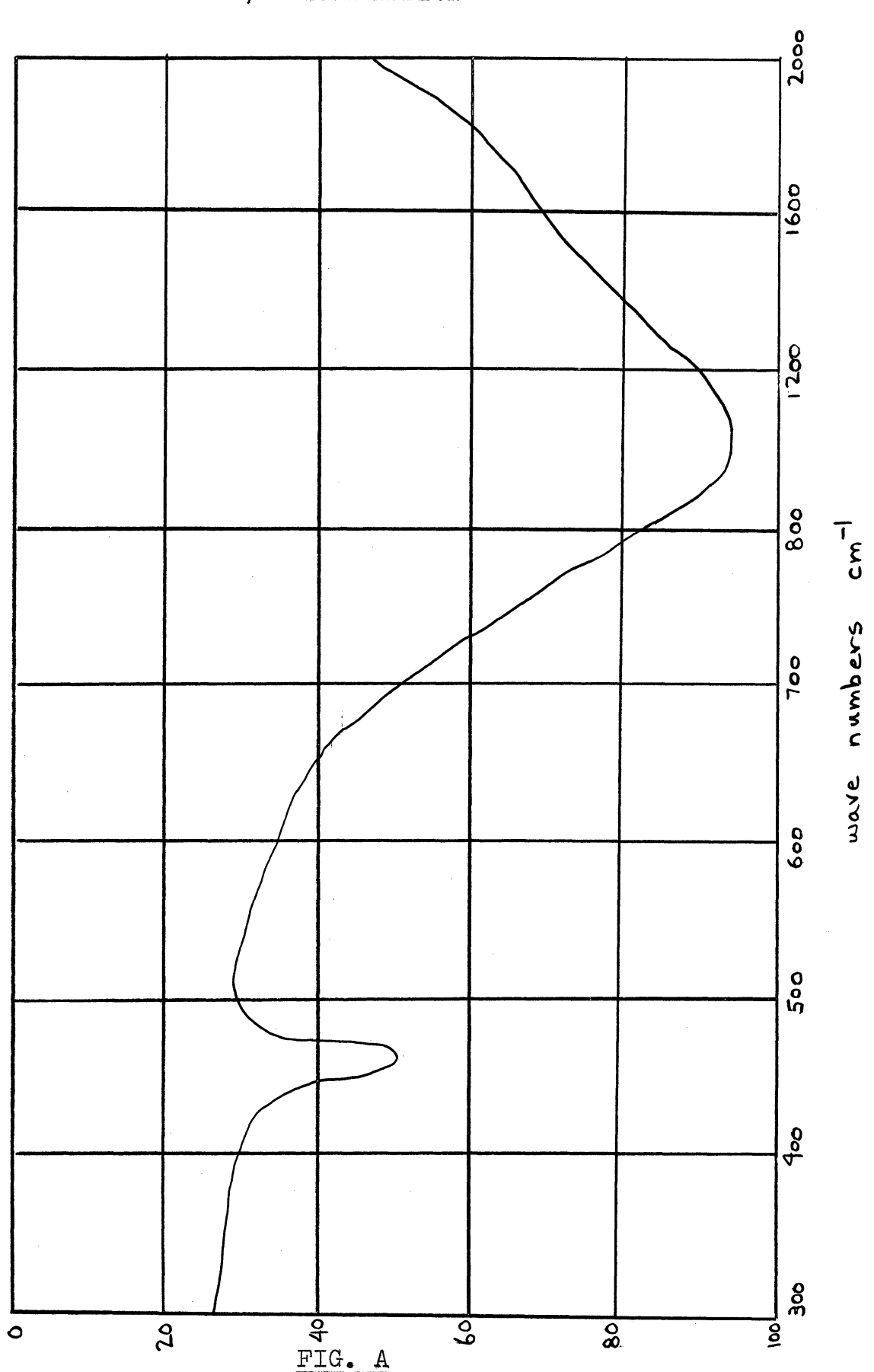
% TRANSMISSION
0
20
40
60
80
100
2000
1600
1200
800
700
600
500
400
300
wave numbers cm⁻¹

FIG. A

11.4, 11.85, and 12.85μ, but the impurities were not identified. The spectrum of a very pure specimen of powdered strontium titanate ($SrTiO_3$) was observed between 2μ and 15μ. (Fig. B) It is identical with that of barium titanate obtained under similar conditions over that region of the spectrum. Noland[1] has recently reported the spectrum of a single crystal of strontium titanate between 1μ and 10.5μ, at which wavelength the extinction coefficient is greater than 100 cm^{-1} and is still increasing. He finds two weak bands near 5.5μ and 7.5μ. These could easily have been missed by us since our effective thickness was much less than the thickness he used. We might add that the spectrum of a single crystal of barium titanate just run in this laboratory by M. Haas shows a weak band at 8μ and a "cut off" near 11.2μ. The spectrum of ilmenite ($FeTiO_3$) has been recorded by Hunt and others[2]. With the exception of a weak band at 100 cm^{-1}, it is also very similar to that of barium titanate.

Apart from impurity bands, there appears to be no difference between the spectrum of barium titanate in the hexagonal and in the tetragonal form over the range 2μ to 15μ. No change was observed in the spectrum of barium titanate

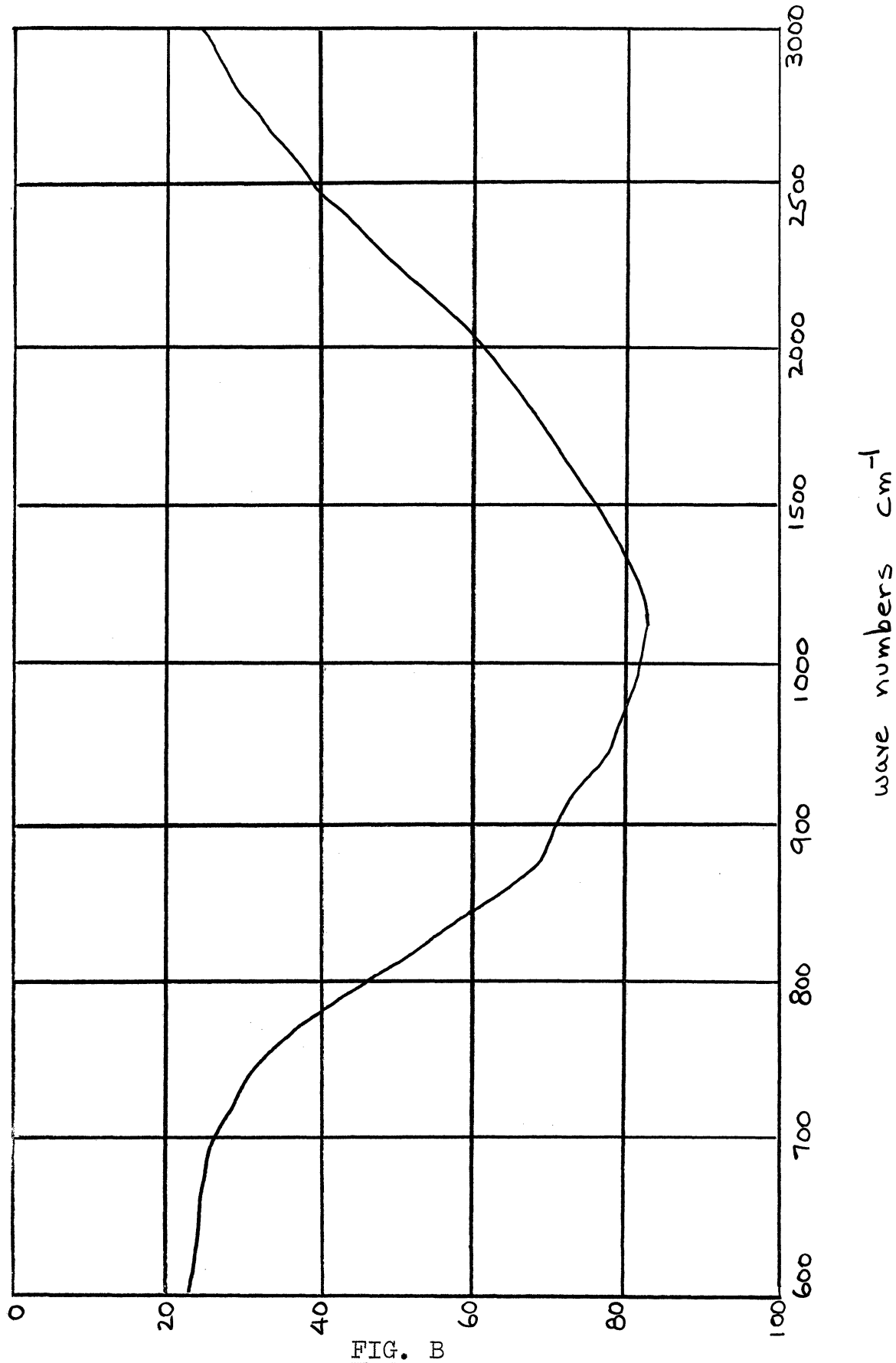
% TRANSMISSION
0
20
40
60
80
100
3000
2500
2000
1500
1000
900
800
700
600
wave numbers cm^{-1}

FIG. B

(ceramic) when heated to 150° C.

The foregoing observations may be considered in the light of recent theories about the ferroelectric character of barium titanate.

Jaynes[3] has predicted from an electronic theory that there should be an infrared absorption at 1000 cm^{-1}. There is definitely no strong absorption band in the neighborhood of 1000 cm^{-1}. Although a few specimens have shown a very weak absorption near 1000 cm^{-1}, this is most probably due to BaO impurity.

Megaw[4] has proposed that the change from the cubic form (above the Curie point of 120° C.) to the tetragonal form corresponds to a change in the character of the bonds round the Ti and O atoms. If this were so, one might expect a change in the spectrum on heating to 150° C. and also differences between the spectra of the tetragonal and hexagonal forms of $BaTiO_3$ since the latter is not ferroelectric. This change should be very marked in the strong band near 600 cm^{-1} since this band (which is common to all titanates and is found also in rutile (TiO_2) is undoubtedly connected with a vibration of the TiO_6 tetrahedra. No such change was observed. It is possible, of course, that changes may have occurred at lower frequencies beyond the range of detection.

This work was sponsored by the U. S. Army Signal Corps under Contract DA 36-039 sc-5581 from the

Squier Signal Laboratory.

R. T. Mara
G.B.B.M. Sutherland
H. V. Tyrell

Randall Physics Laboratory
University of Michigan
Ann Arbor, Michigan

References

1
J. A. Noland, Phys. Rev. 94: 724 (1954)

2
J. M. Hunt, M. P. Wisherd, and L. C. Bonham. Anal. Chem. 22: 1478 (1950)

3
E. T. Jaynes. "Ferroelectricity." Princeton Univ. Press: 69 (1953)

4
H. D. Megaw. Acta Crystallographica 5: 739 (1952)

The above letter contains all of the important fundamental results on barium titanate. The details have already been given in Quarterly Reports 1, 2, 3 and 4 or in the First Annual Report (August 1952).

With regard to TiO_2, there is nothing to add to the work reported in the First Annual Report (August 1952).

IV. B. Diamond, Silicon and Germanium

All of the factual data on diamond, silicon and germanium have been given in Technical Report No. 1 (June, 1953) with one exception. In the summer of 1953, Dr. Harmon Craig of the Institute for Nuclear Studies in Chicago University kindly agreed to make an analysis of diamonds of various types to determine the C^{13}/C^{12} ratio as we thought this might throw light on the cause of anomalous absorption in Type I diamonds. We sent him three diamond chips; one was a strong Type I, one a weak Type I and one a Type II. We have now received the report of his analysis. It turned out that the strong Type I had the lowest C^{13}/C^{12} ratio, while the Type II had an intermediate value of this ratio. This proves that the C^{13} content of diamond is quite unconnected with differences between Type I and Type II diamonds.

Our general conclusions on Diamond at present are contained in the following inset paragraphs which are a copy of an article recently submitted for publication to "Nature".

The Problem of the Two Types of Diamond

Introduction

Exactly twenty years ago, Robertson, Fox and Martin[1] reported the existence of two types of diamond having marked differences in infrared and ultraviolet absorption, in photoconductivity and birefringence. Somewhat later, Raman and Nikalantan[2] reported that many diamonds had extra spots or streaks in their X-ray diffraction patterns. This observation was confirmed by Lonsdale and Smith[3], who reported that extra streaks were characteristic of Type I diamonds and also that in general Type II diamonds appear to be much more mosaic in structure than Type I diamonds. The principal characteristics of the two types of diamond as determined from these early investigations are summarized in Table I.

TABLE I

Characteristic Features of the Two Types of Diamond

Physical Property	Type I	Type II
Infrared Absorption	Bands at 4 to 5μ Absorption 8 to 10μ	Bands at 4 to 5μ None between 8 and 10μ
Ultraviolet Absorption	Complete beyond 3000 A.	Transparent to 2250 A.
X-ray diffraction	Shows extra spots and streaks	Normal
Photoconductivity	Poor	Good
Birefringence	Present	Absent

Subsequently Sutherland and Willis[4] and also Ramanathan showed that Type I diamonds are not uniform

in their infrared absorption, since the extinction coefficient of the 8-10μ band varies very widely from diamond to diamond. Thus the Type II diamond may be regarded as a limiting case in which the value of the extinction coefficient of the 8 - 10μ band has become vanishingly small. A similar gradation has been found in the position of the ultraviolet cut-off and in the intensity of the extra spots in the X-ray diffraction patterns. Thus diamonds may be more satisfactorily classed as extreme Type I, medium Type I, weak Type I and Type II. It should be added that Blackwell and Sutherland[6] have reported two types of Type II diamond, neither of which exhibited any absorption in the 8 - 10μ region but which showed differences in the 3 - 5μ region.

No explanation for these anomalies in the physical properties of diamonds has been yet put forward which has received general acceptance. In an attempt to seek a satisfactory solution of this puzzling phenomenon, we have made an extensive investigation of the infrared and ultraviolet spectra of a selection of diamonds. In a short paper giving an account of some of the early results[6], we suggested that the Type II diamond was a normal pure diamond while all Type I diamonds had some impurity or imperfection in their structure which would account for the anomalies. The purpose of the present note is to present briefly the

main results of our investigations with particular reference to the imperfection theory.

Type I and Type II Diamonds

First, however, it is necessary to consider a little more carefully the distinguishing features of Type I and Type II diamonds. Although any one of the properties listed in Table I has been generally accepted as a reliable guide in distinguishing Type II from Type I diamonds, the parallelism of all the physical properties is not at all satisfactory in classifying Type I as "extreme", "medium", or "weak", and occasionally a diamond classed as Type II on the basis of one physical property would be classified as Type I, if one of the other properties were used. In a paper primarily concerned with possible correlations between the counting properties of diamonds and their crystal texture (as shown by divergent beam X-ray photographs) Grenville-Wells[7] has listed various physical properties of 38 diamonds. Four of these diamonds had a cut-off in the ultraviolet below 2400 A., yet exhibited anomalous extra strong X-ray streaks, i.e. by ultraviolet examination these four diamonds would have been classed as weak Type I but by X-ray streaks as medium or strong Type I. Similarly three diamonds which showed no extra streaks (and would therefore have been classified as Type II) had their ultraviolet cut-off at wavelengths longer than 2830 A.

(indicating that they were medium or strong Type I). Through the courtesy of Dr. Grenville-Wells, we have been able to examine the infrared spectra of 13 of these 38 diamonds. We have found that in every case there is excellent correlation between the infrared and ultraviolet method of classifying diamonds, but very poor correlation between the infrared and X-ray method. In this connection it should also be added that the observations of Grenville-Wells has shown that mosaic character cannot be reliably correlated with Type II diamonds as originally suggested by Lonsdale[3].

There is, therefore, strong evidence that the same cause operates in producing the extra absorption found in the infrared and ultraviolet spectra of all Type I diamonds but that additional factors may be the cause of the extra streaks and of the mosaic character found in the X-ray photographs of certain diamonds. In view of this, we propose to use a modified nomenclature in the future for the description of Type I and Type II diamonds. A diamond which is found to be Type I (or Type II) by spectroscopic means will be denoted by IS (or IIS) while a diamond classified by X-ray methods will be denoted by IX (or IIX). The spectroscopic symbol can be elaborated to read Sir or Suv depending on whether infrared or ultraviolet radiation was used in making the classification; similarly, the X-ray symbol should be

modified to read Xl or Xd to indicate whether the diamond was classified by extra streaks on a Laue photograph or mosaic character as shown by a divergent beam technique. Possible extensions of this notation by using combinations of the X and S symbols together with e, m and w to denote extreme, medium and weak are sufficiently obvious and need not be discussed here.

The distinctions just drawn between the various Type I and Type II diamonds are important in what follows, because in this communication we shall restrict our discussion to IS and IIS diamonds. It appears to us that at least some of the confusion in the diamond problem can be eliminated in this way. In other words, there are several Type I and Type II diamond problems and we propose to start with the IS and IIS types, since the classification by infrared and ultraviolet absorption has been found (by the examination of several hundred stones) to give very consistent results.

We may begin by considering what would be predicted for the ultraviolet and infrared spectra of diamond assuming the Bragg structure and the current theories of molecular spectra.

Ultraviolet Absorption of an Ideal Diamond

From the examination of the ultraviolet spectra of large numbers of hydrocarbons, it has been found

that only those hydrocarbons which contain a double or triple carbon-carbon bond exhibit absorption at wavelengths longer than 2000 A. Since diamond presumably contains only single bonds, its ultraviolet cut-off might be expected to be below 2000 A. Since no IIS diamonds have been found with a cut-off below 2200 A., it appears at first sight as if all diamonds are anomalous in their u.v. absorption with IIS less anomalous than IS. However, Klevens and Platt[8] in an investigation of the ultraviolet spectra of branched saturated hydrocarbons have shown that as the degree of branching increases, the edge of the ultraviolet cut-off moves to longer wavelengths, e.g. from 1715 A. in n-pentane, to 1795 A. in 2,2,3,3-tetramethylpentane. One might, therefore, anticipate that diamond (which from this point of view resembles an extremely highly branched large hydrocarbon molecule) would have its ultraviolet cut-off in the neighborhood of 2000 A. In order to test this hypothesis, we have examined the ultraviolet spectrum of adamantane ($C_{10}H_{16}$) which consists of four "fused" cyclohexane rings and which would yield diamond if it ever could be "polymerised." The ultraviolet cut-off of adamantane, while not as sharp as that of a IIS diamond, is indeed very close to 2200 A. We should add that Herman[9] has recently made a theoretical calculation of the separation between the filled and unfilled electronic energy

levels of diamond and obtained a value of approximately 6 electron-volts. This corresponds to an absorption edge of about 2050 A. We therefore conclude that the IIS diamonds have perfectly normal ultraviolet absorption and that only the IS diamonds are anomalous.

Infrared Absorption of an Ideal Diamond

From investigations on the infrared absorption spectra of hydrocarbons, the force constants involving carbon-carbon bonds are sufficiently accurately known to make it certain that the fundamental frequency spectrum of the diamond lattice must extend from about 1400 cm^{-1} (7.1μ) to about 300 cm^{-1} (33μ). The exact distribution of the normal modes over this range is a much more difficult problem but calculations have been made by Smith[10] which give reasonable agreement with the observed second order Raman spectrum, and her results can be regarded as a very good first approximation to the true distribution. It is necessary to consider next to what extent these frequencies may be expected to be active in absorption. Using the results of Teller[11] and Lifshitz[12], it can be shown that none of the fundamental frequencies should be active in absorption but that combinations of fundamentals may give rise to absorption.

Now IIS diamonds exhibit no absorption between 1800 cm^{-1} and 100 cm^{-1} (i.e. the fundamental region) but do have bands between 3500 cm^{-1} and 1800 cm^{-1}

(i.e. the region of combination frequencies). Thus IIS diamonds are completely normal in their infrared as well as their ultraviolet absorption.

Problem of the IS Diamonds

The conclusion that IIS diamonds are perfectly normal in their optical absorption properties is an important one. The problem of the IS and IIS types of diamond is now reduced to the problem of why IS diamonds show anomalous absorption. A few years ago, two of us suggested[6] that the extra absorption found in IS diamonds might be due to impurity centres in diamond. The exact nature of these was not specified. Impurity centres may consist of 1) foreign atoms, 2) missing carbon atoms, or 3) carbon atoms which are not in the same electronic state as the majority of carbon atoms in the diamond lattice. We may now consider what the effects of such impurity centres would be on the absorption spectrum of diamond.

a) Ultraviolet Spectrum

It is now well established that chemical impurities in silicon and germanium cause the edge of the main absorption band in these elements to move to longer wavelengths[13]. Thus the shift of the absorption edge from 2250 A. in IIS diamonds to 3000 A. (or even further) in IS diamonds could be due to chemical impurities. The effect of missing carbon atoms on the ultraviolet spectrum is not so easy to predict,

but, in general, lattice defects of this type may be expected to decrease the gap between the ground state and the lower edge of the first band of energy levels. Thus the observations are probably also consistent with this second type of impurity centre. The third type of impurity centre might also be expected to cause a shift of the absorption edge to longer wave-lengths, but in addition might be expected to give rise to discrete lines superimposed on the continuous absorption. Such discrete lines are observed and we have been able to prove that certain of these lines are closely correlated with certain infrared absorption bands in the range below 1800 cm^{-1} (cf. (2) below).

We may conclude that the extra absorption shown by IS diamonds in the ultraviolet can be readily accounted for in a qualitative manner by an impurity theory and that, of the three types of impurity centre considered, that arising from carbon atoms in an abnormal state seems most probable.

b) Infrared Spectrum

Anything which destroys the centre of symmetry midway between each neighboring pair of carbon atoms in the ideal diamond lattice can cause absorption to occur in the region of fundamental frequencies. Thus any of the three varieties of impurity centre considered could conceivably account for absorption by IS diamonds in the region below 1800 cm^{-1}. Before

discussing which seems most probable, we shall summarise the most important results of our investigations on the infrared spectra of IS diamonds.

(1) Absorption maxima of variable intensity have been found in IS diamonds at the following frequencies below 1800 cm^{-1}: 1540, 1520, 1426, 1372, 1332, 1282, 1203, 1171, 1093, 1003, 780, 480 and 328 cm^{-1}. No absorption was found between 300 cm^{-1} and 100 cm^{-1}. All but two of these bands appear to fall into two groups (as shown in Table II) in the sense that the bands in each group always occur together and have the same relative intensity but there is no correlation between the bands in the separate groups. The two maxima near 1530 cm^{-1} have not so far been correlated with either group, but this may be due to the difficulty of making accurate intensity measurements on these weak bands. Many of the Group B bands (e.g. at 1426, 1372, 1332 and 328 cm^{-1}) are very sharp. All the Group A bands are broad.

TABLE II

Distribution of the Absorption Bands of IS Diamonds

Group A	Group B
cm^{-1}	cm^{-1}
1282	1426
1203	1372
1093	1332
480	1171
	1003
	780
	328

(2) It has been found that as the intensity of the Group A bands increases, the cut-off wavelength in the ultraviolet moves to longer wavelengths and the intensity of an ultraviolet line at 3157 A. increases. However, in IS diamonds containing Group B bands, the intensity of this group of bands is independent of the position of the ultraviolet cut-off, but is correlated with the intensity of an ultraviolet absorption line at 4155 A.

(3) Following the methods of Smith[10], we have calculated the branches of the vibration spectrum of the diamond lattice and have been able to explain the high frequency (>1800 cm^{-1}) bands of IS and IIS diamonds in terms of allowed combinations. The Group A bands in the low frequency (<1800 cm^{-1}) spectrum of IS diamonds can also be accounted for in this way, but most of the Group B bands cannot be associated with calculated maxima for the ideal diamond lattice.

(4) When IS diamonds are heated to 400° C., the only detectable change in the infrared spectrum (between 4000 and 700 cm^{-1}) is a decrease of about 30% in the intensity of the 1372 cm^{-1} band. This band also moves to lower frequencies as the temperature increases, the temperature coefficient being 1 cm^{-1}/50° C. Diamonds (IS and IIS), which had been heated to 1700° C. and were re-examined at room temperature, showed no change in infrared spectrum.

(5) The infrared absorption bands of IS diamonds show no dichroic effects in regions where optical birefringence is observed.

(6) Irradiation of IIS diamonds by neutrons, deuterons and x-rays has so far failed entirely to produce any of the absorption bands characteristic of IS diamonds. Neutron irradiation appears to give rise to the formation of graphite. Deuteron irradiation caused color changes in the surface layers (green for a IIS and brown for a IS diamond).

(7) There is no correlation between variations in the C^{13}/C^{12} ratio in diamonds and the intensity of the characteristic IS bands.

It is clear from the foregoing results that there is probably more than one cause for the appearance of anomalous absorption in IS diamonds, since the absorption bands fall into at least two classes which exhibit different properties. Moreover, part of the absorption can be confidently assigned to the activation of normally forbidden frequencies of the ideal diamond lattice but some of the bands appear to be due either to chemical impurities or to carbon atoms in an abnormal state. Isotopic effects cannot account for the anomalous absorption. Since deuteron irradiation fails to convert a IIS into a IS diamond, it seems unlikely that vacant sites are the cause of the IS anomalies.

Conclusions

Our present conclusion is that carbon atoms in an abnormal state and chemical impurities probably both contribute in varying degrees to produce IS diamonds. If some carbon atoms exist in a state which enables them to form double bonds in IS diamonds, then the bands near 1530 cm^{-1} could be due to the vibration of carbon-carbon double bonds in an unsymmetrical environment, and the movement of the ultraviolet absorption edge towards 3000 A. is consistent with the introduction of a few conjugated double bonds into the structure. Since graphite is a more stable form of carbon than diamond, it is tempting to consider that in IS diamonds some parts of the structure have gone part way towards graphite. However, the neutron irradiation experiments seem to produce graphite without giving the typical IS features as an intermediate stage. With regard to chemical impurities, it should be realised that there is very good spectroscopic evidence[14] for the presence of many impurities in the average diamond and some evidence[14] (although much weaker) that IIS diamonds are less impure than IS diamonds. This is a point on which we hope to conduct further investigations. The appearance of some very narrow absorption bands in Group B (which do not seem to belong to the diamond lattice) is most easily explained by

attributing them to the presence of chemical impurities.

What does seem certain from these investigations is that Type I diamonds (specifically IS diamonds) are imperfect. This is an unexpected result, since in our experience all large diamonds of gem stone quality are always Type I diamonds. While some very small Type II diamonds are perfect octahedra, all the large Type II diamonds which we have examined are very far from any of the ideal crystalline forms of diamond (octahedron, cube, etc.) and in fact, usually exhibit a layered structure with highly irregular faces and fractured edges. It would almost appear as though a large single crystal having the ideal Bragg structure is unstable and requires certain impurity centres to be incorporated to give stability. The beneficial effect of impurities in the growing of large single crystals is well known to workers in that field[15].

A full account of this work is now being prepared for publication in a more appropriate journal.

Acknowledgements

We are most grateful for the loan of diamonds from Industrial Distributors Ltd., Messrs. Triefus and Co., Lazare Kaplan and Sons Inc., the late Professor W. T. Gordon, Dr. K. Lonsdale, Professor

C. B. Slawson, Dr. W. C. Parkinson and Dr. Grenville-Wells. We are very much indebted to Dr. Harmon Craig for making the C^{13}/C^{12} analysis for us. Some of the later phases of this work received valuable financial aid from the U.S. Army Signal Corps under Contract DA 36-039 sc-5581.

G.B.B.M. Sutherland
D. E. Blackwell [a]
W. G. Simeral [b]

Randall Physics Laboratory
University of Michigan
Ann Arbor

References

1) Robertson, R., Fox. J. J. and Martin, A. E. Phil. Trans. Roy. Soc., A. 232:463 (1934)

2) Raman, C. V. and Nikalantan, P. Proc. Ind. Acad. Sci., 11:379 (1940)

3) Lonsdale, K. and Smith, H. Nature, 148:112 (1941)

4) Sutherland, G.B.B.M. and Willis, H. A. Trans. Faraday Soc., 41:289 (1945)

5) Ramanathan, K. G. Proc. Ind. Acad. Sci., 24:137 1946

6) Blackwell, D. E. and Sutherland, G.B.B.M. J. Chim. Phys. 46:9 (1949)

7) Grenville-Wells, H. J. Proc. Phys. Soc., 65:313 (1952)

8) Klevens, H. B. and Platt, J. R. J. Am. Chem. Soc., 69:3055 (1947)

9) Herman, F. Phys. Rev., 88:1210 (1952)

10) Smith, H. M. F. Phil. Trans. Roy. Soc., A. 241:105 (1948)

11) Teller, E. Hand. und Jahrbuch der Chem. Physik, 9, II:161 (1934)

a. Now at the Solar Physics Observatory, Cambridge University.
b. Now with E. I. duPont de Nemours Co., Wilmington, Delaware.

12) Lifshitz, I. M. J. of Physics (U.S.S.R.), 7:215 & 249 (1943); ibid, 8:89 (1944)

13) Fan, H. Y. and Becker, M. in "Semi-Conducting Materials", Butterworth Ltd., London (1951), pp. 132

14) Chesley, F. G. Amer. Min., 27:20 (1942)

15) Buckley, H. E. "Crystal Growth", John Wiley (1951)

A suitable condensation and revision of the full account of the work on diamond, silicon and germanium given in Technical Report No. 1 (June 1953) is gradually being prepared for publication.

One other piece of work related to diamond may be mentioned at this point. Dr. Venkatarayudu has shown that in the case of crystals which possess a centre of symmetry (diamond is such a crystal) the rule of mutual exclusion breaks down for combination frequencies although it is still true for fundamentals. This work has been published in the Journal of Chemical Physics and a copy is given in Appendix I of this report.

IV. C. Brucite

A full account of all the experimental work on Brucite done in the period covered by this report has already been given in Technical Report No. 2 (October 1954).

Part of this work has already been published in the Journal of the Optical Society. This is attached to this report as Appendix II.

IV. D. Micas

After making a general survey of the spectra of muscovite,

biotite, phlogopite (natural and synthetic), lepidolite, and zinnwaldite (which has been described in the first Annual Report of August 1952), attention was directed to the identification of bands characteristic of the OH group other than the well-known 3μ absorption. The results of this work were rather inconclusive and were reviewed in the second Annual Report (June 1953). We therefore concentrated our efforts on a thorough investigation of the 3μ absorption in muscovite and biotite using polarised radiation. Brief reports of this work have been given in Quarterly Reports 9 (December 1953) and 10 (March 1954) and in this section of the report we shall describe the detailed investigations made on the 3μ bands of muscovite and biotite and the resulting conclusions reached regarding the location of the hydrogen atoms in these micas.

The Location of the Hydrogen Atoms in Muscovite and Biotite from Investigations on the Dichroism of Absorption Bands in the 3μ Region

Tsuboi[1] has recently reported a similar investigation on muscovite, but his theoretical treatment of the problem is incomplete, and our experimental data are considerably superior. Vergnoux, Theron and Pouzol[2] have also attempted to locate the hydrogens in muscovite from studies on its birefringence. The results of this earlier work will be discussed later when comparison can be made with our results. It is convenient to start by describing briefly the results of X-ray studies on the structure of the micas in order to understand clearly the atomic framework into which the hydrogen atoms have to fit.

The first application of X-ray analysis to the structure of mica was made by Mauguin[3]. Some years later Pauling[4] described the general structural scheme, but the only complete X-ray analysis of a mica structure appears to be that of Jackson and West[5] on muscovite. From a study of powder photographs of several micas, Nagelschmidt[6] concluded that there are two general classes into which all micas fall, viz. (a) the muscovite type and (b) the phlogopite-biotite type. Following Brindley[7], these two types may be described in terms of two structural units which we shall call T units and O units.

The T unit (or tetrahedral layer) is composed of linked SiO_4 tetrahedra (Fig. 1) in which approximately one-fourth of the Si^{++++} ions are replaced by Al^{+++} ions. The O unit (or octahedral layer) consists of two plane sheets of O^{--} and OH^- ions arranged in hexagons of O^{--} around each OH^-. (Fig. 2) Between these sheets is a plane of ions which are located at the centers of octahedra formed by joining the vertices of two triangles such as A B C and A'B'C', one of which belongs to each sheet. However, only two-thirds of the available centers are occupied by Al^{+++} in the case of muscovite (Fig. 3A), whereas, in phlogopite Mg^{++} ions occupy all of the available centers (Fig. 3B), while in biotite, some of the Mg^{++} ions in the phlogopite structure are replaced by Fe^{++} ions (Fig. 3C).

The way in which these two units are combined to give a typical mica is illustrated in Fig. 4, which according to Bragg[8], gives three views of the conventional crystallographic unit cell. Four T units are arranged as shown, i.e. in two

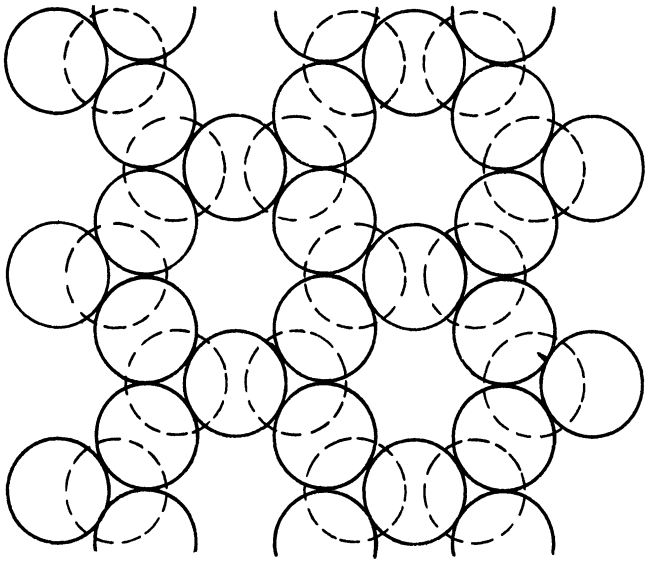

Fig. 1. Tetrahedral Layer, Composed of Linked SiO_4 Tetrahedra. The circles Represent Oxygen Atoms; the Silicon Atoms at the Centers of Tetrahedra are not shown

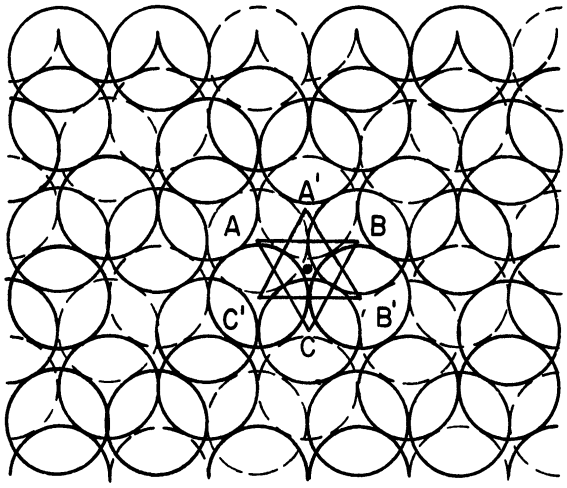

Fig. 2. Octahedral Layer. Composed of Two Plane Sheets of O^{--} and OH^{-} ions. The Red Circles Represent One Sheet, Black Circles Represent Another Sheet. Circles in Full Line Represent O^{--}, in Dotted Line Represent OH^{-}; • Represents Center of One of the Octahedra

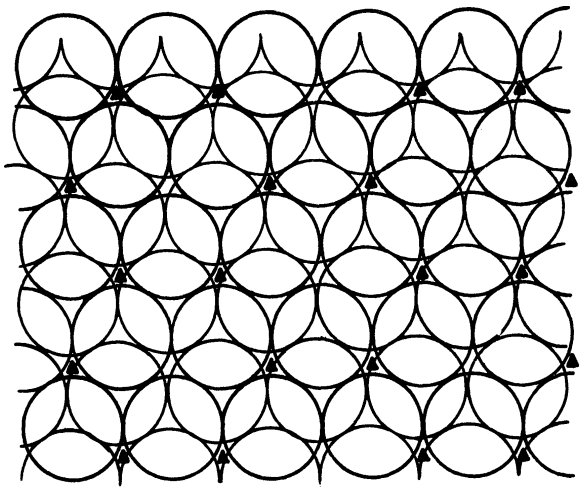

Fig. 3 A. Octahedra of Muscovite, ▲ AL^{+++}

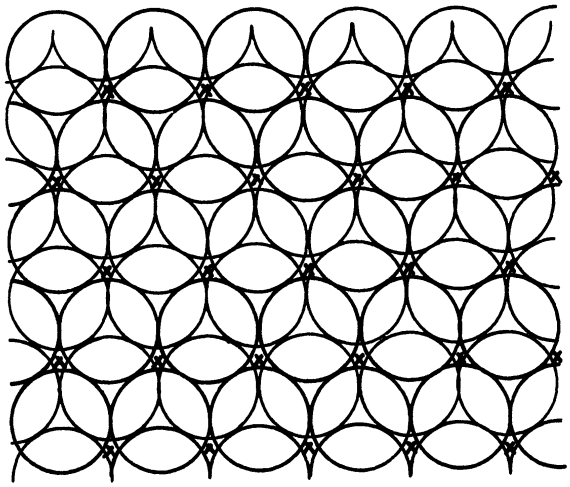

Fig. 3 B. Octahedra of Phlogopite, x Mg^{++}

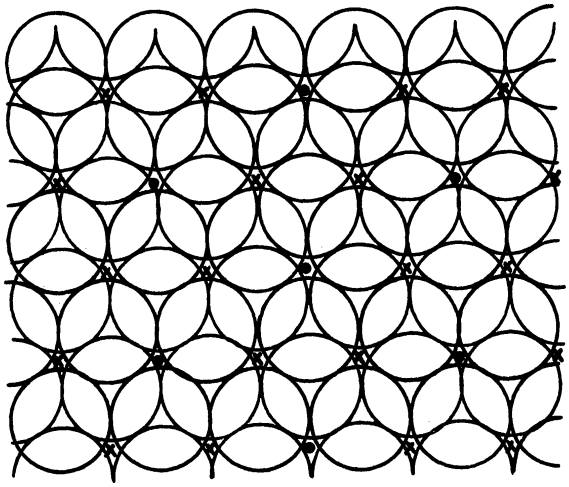

Fig. 3 C. Octahedra of Biotite, • Fe^{++}, x Mg^{++}

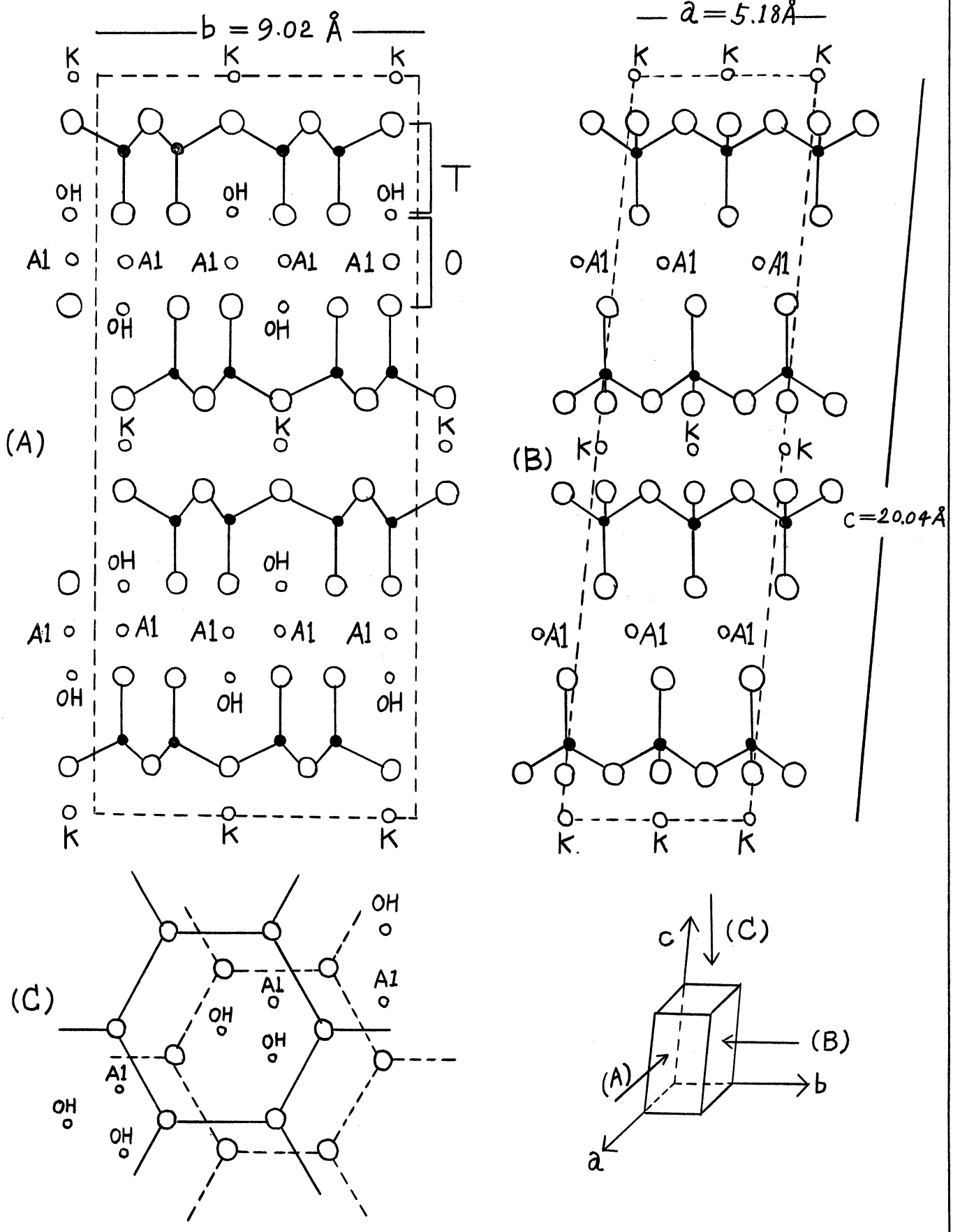

Fig. 4 The Crystal Structure of Muscovite. (A) Projected on a plane normal to a-axis. (B) Projected on a plane normal to b-axis. (C) Projected on cleavage plane.

pairs with the vertices of the tetrahedra pointing inwards towards one another; the two pairs are separated from one another by a plane of K^+ ions (Fig. 4A). The O units consist of the O^{--} ions of the vertices of the SiO_4 tetrahedra together with OH^- ions at the center of each hexagon of O^{--} ions and the intervening layer of metallic ions (Figs. 4A and 4C)

The muscovite structure, in which only two-thirds of the octahedral centers are occupied is known as dioctahedral, while biotite and phlogopite in which all of the octahedral positions are occupied are referred to as trioctahedral.

It should be noted that the crystallographic unit cell illustrated in Fig. 4 contains 8 OH^- ions although it should be remembered that some of these OH^- ions may be replaced by F^- ions in natural phlogopite. In synthetic phlogopite, all of the OH^- ions have been replaced by F^- ions.

Symmetry Properties and Selection Rules for OH Vibrations in Muscovite

Let us now restrict our attention to these 8 OH^- ions and consider a somewhat different view of the crystallographic unit cell (Fig. 5) in which the c axis is horizontal, and only the oxygens of the OH^- ions are shown. The space group of muscovite has been determined by X-ray analysis[5] to be C_{2h}^6. The symmetry elements are:- (Fig. 5):

(1) A twofold (C_2) axis parallel to the b axis through the center of the unit cell

(2) Two centers of symmetry (i) located symmetrically with

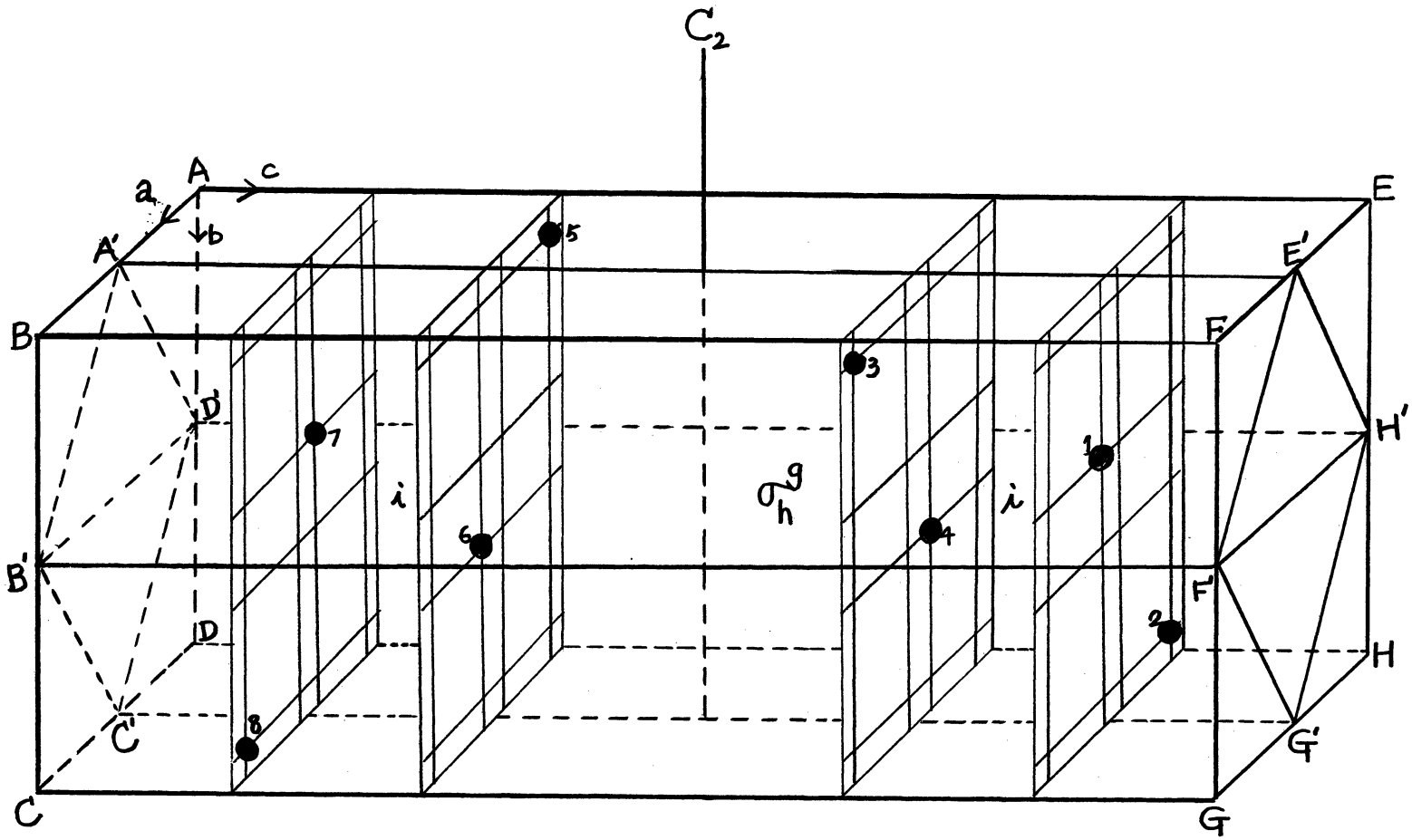

FIGURE 5. A B C D E F G H ----- Crystallographic Unit Cell of Muscovite
A'B'C'D'E'F'G'H'----- Bravais Unit Cell of Muscovite
1,2,3,4,5,6,7,8 -----. Eight OH groups in one Crystallographic Unit Cell

C_2 ----------Two Fold Axis

σ_h^g (B'D'F'H') --------Glide Plane

i ----------Center of Symmetry

a, b, c ---Crystallographic Axes

respect to the two groups of O atoms in each half of the unit cell

(3) A glide plane (σ_h^g) bisecting the unit cell horizontally i.e. B'D'F'H'.

For the space group C_{2h}^6, the Bravais unit cell (which determines the infrared selection rules) is smaller than the conventional crystallographic unit cell we have been discussing. The Bravais unit cell is given by A'B'C'D'E'F'G'H' and contains only 4 OH^- ions. X-ray analysis has located the oxygen nuclei and our problem is to consider possible positions of the hydrogen nuclei consistent with this space group. It is, of course, only necessary to determine the location of any one of the four hydrogens since the positions of the other three are then determined by the symmetry operations of the space group.

Since the mass of the hydrogen is so much less than that of the oxygen and the binding forces between these two atoms are much greater than those between either of them and any other atom in the lattice, we may consider the vibrations of the OH^- ions as falling into three classes:

a) Stretching vibrations of the OH^- ions in which the hydrogens move along the lines of the OH bonds

b) Deformation vibrations of the OH^- ions in which the hydrogens move at right angles to the OH bonds

c) Motions of the OH^- ions in which the OH^- ions move as rigid units.

Using the methods of group theory[9], the 24 fundamental modes of vibration of the four OH^- ions can be put into 4

symmetry species as shown in Table I, in which n is the number of stretching vibrations, D of deformation vibrations (pseudo rotations of the OH^- ions) and T of translational motions. These last are essentially lattice vibrations involving the other heavy atoms in the structure and need not be considered in what follows. We shall also ignore the deformation vibrations in this section of the report and concentrate on the stretching vibrations which are responsible for the absorption band common to all micas (except synthetic phlogopite) near 2.8μ.

TABLE I

C_{2h}^6	E	C_2	i	σ_h^g	n	D	T	IR	R
A_g	1	1	1	1	1	2	3	f	p
A_u	1	1	-1	-1	1	2	3	p	f
B_g	1	-1	1	-1	1	2	3	f	p
B_u	1	-1	-1	1	1	2	3	p	f

p = permitted, f = forbidden, IR = Infrared, R = Raman

Accerding to Table I there are 4 OH stretching modes, two of which (A_u, B_u) are permitted in infrared absorption, the other two (A_g, B_g) being permitted only in Raman spectra. The physical character of the A_u and B_u modes is illustrated in Fig. 6, which shows projections of the unit cell perpendicular bz and az planes. The z axis is perpendicular to the a and b axes and thus makes an angle of 5° with the c axis. It will be observed that the change of electric moment for the A_u mode is

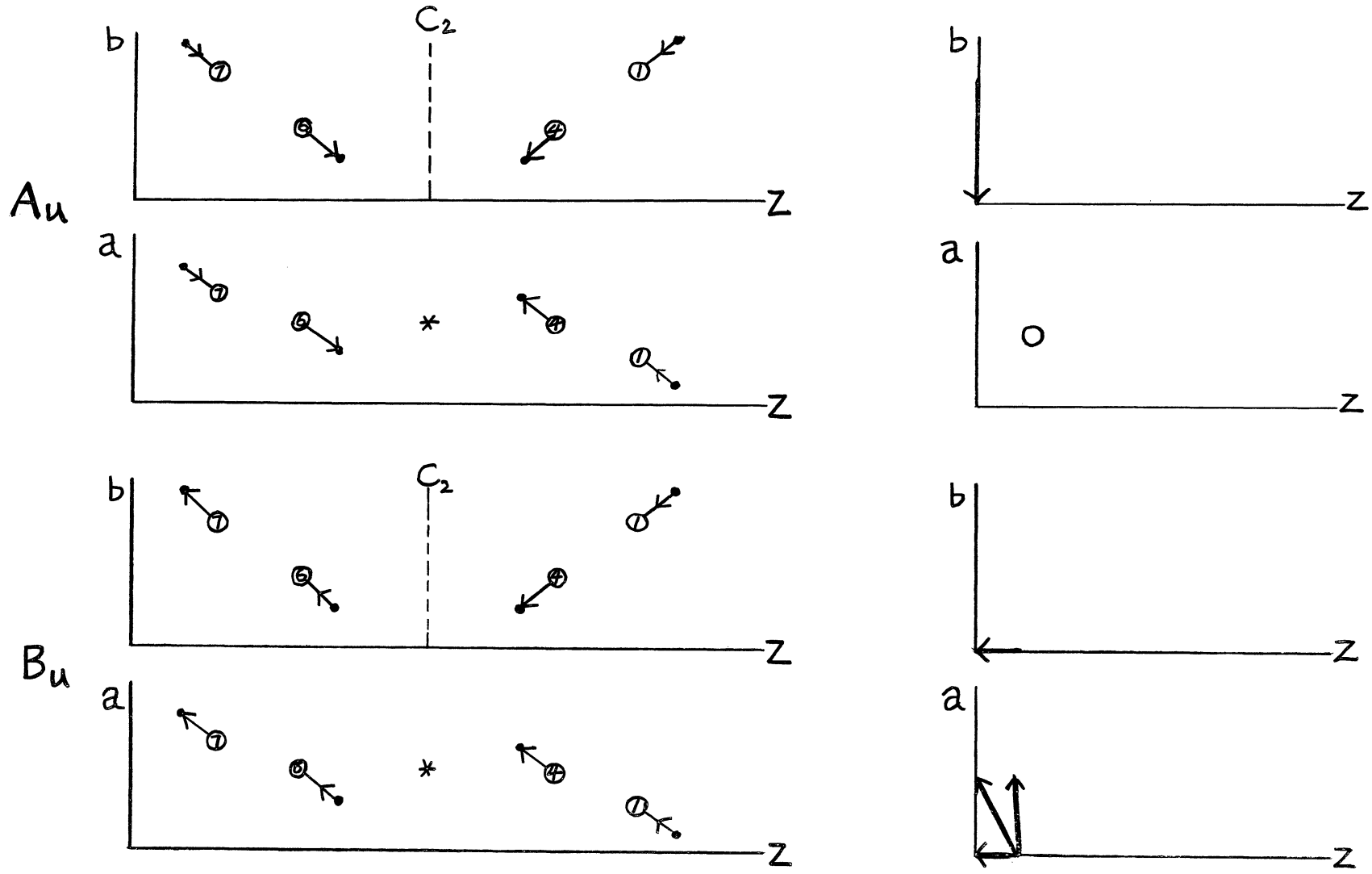

Fig. 6. MODES of OH Stretching Vibrations of Muscovite and the Corresponding Electric Moment Change.

parallel to the b axis, whereas that for the B_u mode has one component parallel to the z axis and another component parallel to the a axis. It will be observed that these two modes of vibration can be regarded as motions in which the modes for the two ions in the right and left hand halves of the unit cell are identical but are combined in phase and out of phase with one another. Since the distance between the two oxygens in either half of the unit cell is much less than the distance between any two oxygens in opposite halves of the unit cells, we shall assume that A_u and B_u give rise to a single absorption band, i.e. the separation between the A_u and B_u frequencies is too small to be observed experimentally. This assumption is justified by the observation that muscovite only exhibits one OH stretching frequency at 2.75μ even when examined with a prism of LiF.

The position of any one of the four hydrogen atoms can be defined by 3 parameters, viz. a_o, b_o, and z_o its coordinates with reference to the associated oxygen atom measured respectively along the a, b and z axes. We have assumed in Fig. 6 that the hydrogen atoms point away from one another but these directions could all be reversed and there will be a corresponding ambiguity in our final results.

It is now possible to write down an expression for the absorption coefficient of the 2.75μ absorption band as a function of a, b, z (the corresponding displacement coordinates) and the angle of refraction r which the refracted ray makes with the z axis. Two orientations of the crystal should be

considered (Fig. 7):

(A) The electric vector of the incident radiation is kept perpendicular to the b axis and the crystal is tilted through a range of angles about the b axis.

In this case the absorption coefficient α_b should be proportional to $(4a \cos r + 4z \sin r)^2$. This absorption is due solely to the B_u species.

(B) The electric vector of the incident radiation is kept perpendicular to the a axis and the crystal is tilted through a range of angles about the a axis.

In this case the absorption coefficient α_a should be proportional to $(4b \cos r)^2 + (4z \sin r)^2$. This absorption is partly due to the A_u and partly to the B_u species.

Experimental Results on Muscovite

The results described below were obtained on a sheet of mica about 3μ thick using a Model 21 Perkin-Elmer Infrared Spectrometer with a rock salt prism. The directions of the a and b axes were determined by the optical method[10].

Using a silver chloride polariser, the absorption of plane polarised radiation by the muscovite was investigated between 2 and 3.5μ (1) with the b axis vertical for various angles of tilt about the b axis, (2) with the a axis vertical for a similar range of angles of tilt about the a axis. A typical series of spectra thus obtained is shown in Fig. 8. The results are summarized in Table II in which the first column

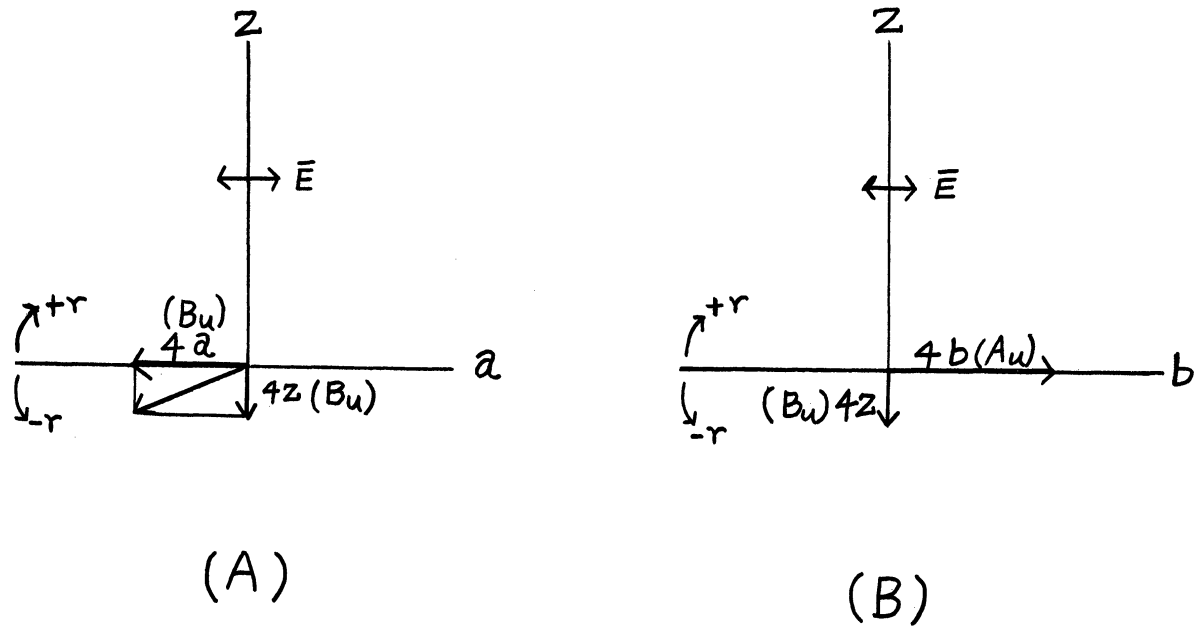

Fig. 7 Orientations of Muscovite and Electric Moment Change of OH Stretching Vibrations. (A) b Axis perpendicular to plane of paper, crystal tilted about b Axis, Incident E Vector perpendicular to b Axis. (B) a Axis perpendicular to plane of paper, crystal tilted about a Axis, Incident E Vector perpendicular to a Axis.

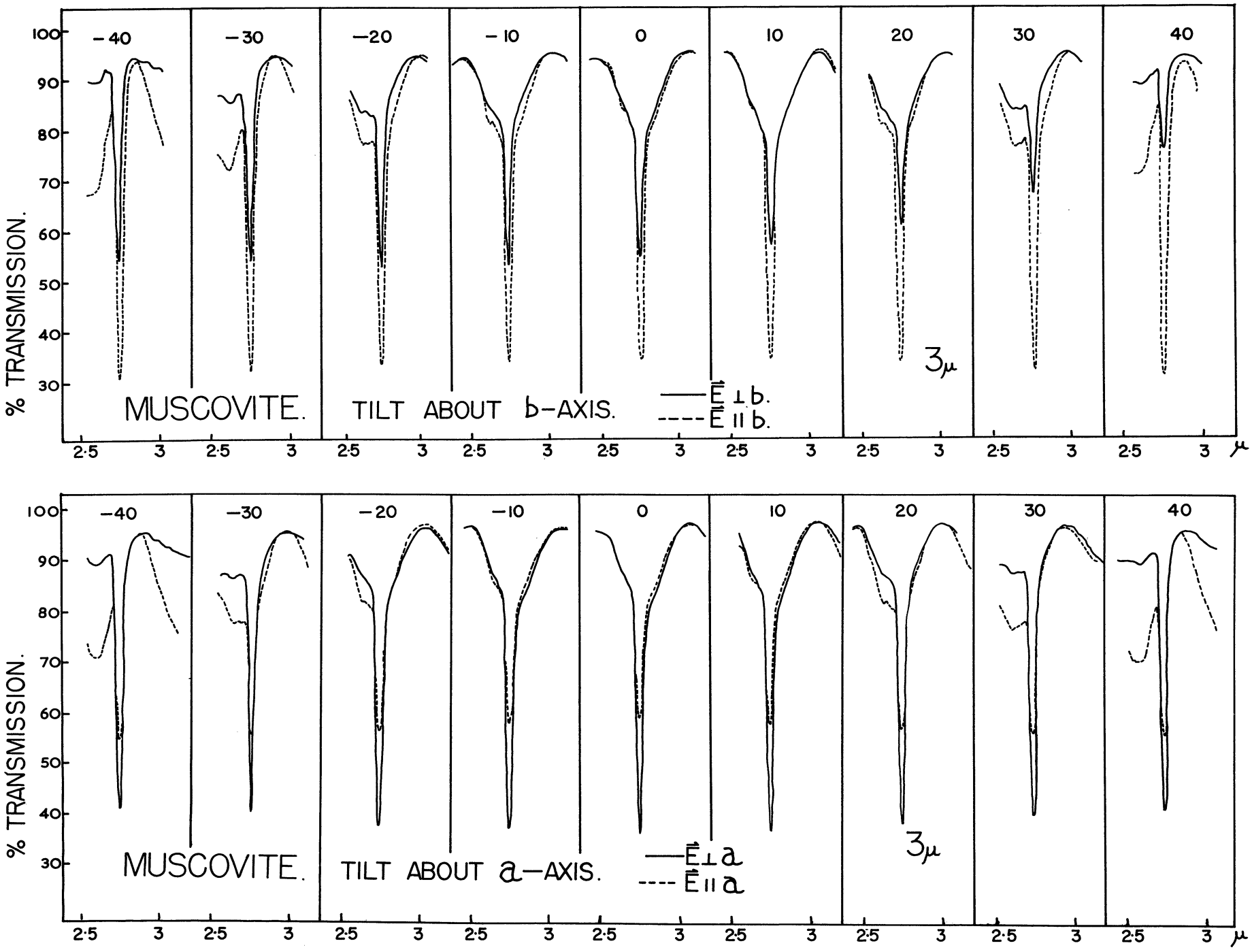

Fig. 8. Spectra of Muscovite

TABLE II

Tilted about b axis

		$\bar{E} \perp b$			$\bar{E} \parallel b$		
i	r	T	α_b (Obs.)	α_b (Cal.)	T	α_b° (Obs.)	α_b° (Cal.)
-40°	-23°55'	81.3	.189	.182	38.6	.870	.889
-30°	-18°23'	78.9	.225	.225	40.7	.853	.889
-20°	-12°28'	75.6	.273	.272	41.6	.856	.889
-10°	- 6°17'	72.2	.324	.318	41.0	.887	.889
0°	0	68.9	.372	.360	41.0	.892	.889
+10°	+ 6°17'	67.4	.392	.396	41.4	.877	.889
+20°	+12°28'	64.5	.428	.423	41.5	.859	.889
+30°	+18°23'	62.3	.449	.441	39.2	.889	.889
+40°	+23°55'	60.3	.462	.449	37.2	.904	.889

Tilted about a axis

		$\bar{E} \perp a$			$\bar{E} \parallel a$		
i	r	T	α_a (Obs.)	α_a (Cal.)	T	α_a° (Obs.)	α_a° (Cal.)
-40°	-23°55'	43.1	.769	.758	68.0	.352	.360
-30°	-18°23'	42.5	.812	.810	70.6	.330	.360
-20°	-12°28'	42.1	.844	.852	71.2	.332	.360
-10°	- 6°17'	42.0	.862	.879	71.0	.340	.360
0°	0	41.2	.887	.889	70.4	.351	.360
+10°	+ 6°17'	42.3	.855	.879	70.0	.354	.360
+20°	+12°28'	42.9	.826	.852	71.2	.332	.360
+30°	+18°23'	42.9	.803	.810	70.8	.328	.360
+40°	+23°55'	42.3	.786	.758	69.6	.331	.360

gives the angle of incidence (i), the second gives the angle of refraction (r), the third gives the percent transmission (T), and the fourth gives the absorption coefficient (α) computed from T by the equation

$$\frac{\alpha}{\cos r} = \log_e \frac{100}{T}$$

The refractive index was assumed to be 1.585 since it can be shown that for these angles of incidence, the effects of double refraction can be ignored.

It will be observed that the absorption coefficients α_a° and α_b° are very nearly constant for all angles. We define α_a° and α_b° as the absorption coefficients corresponding to α_a and α_b when the electric vector is parallel to the axis of tilt. It can be readily shown that α_b° should be proportional to $(4b)^2$ and α_a° should be proportional to $(4a)^2$. This is a test of our experimental error, since the coefficient should be constant for such a series of observations. However, when the electric vector is perpendicular to the axis of tilt, α varies with i. Using all the data from normal incidence, we have (according to the expressions above)

$$(4a)^2 = 0.36 \quad \text{and} \quad (4b)^2 = 0.89$$

giving $\quad 4a = 0.6 \quad$ and $\quad 4b = 0.943.$

Using next the data with $i = -30°$, $r = -18°23'$ for tilt about b and $\bar{E}$ perpendicular to b we get

$$(4a \cos 18° 23' - 4z \sin 18° 23')^2 = 0.225$$

giving $\quad 4z = 0.3.$

If now these values of a, b and z are substituted in the above

expressions for α_a and α_b we obtain predicted values for α_a and α_b for all other angles. These values are given in the fifth columns of Table II. It will be seen that the agreement is very satisfactory.

It will be noticed that in the above computations z was assumed positive. This is equivalent to saying that the two hydrogens in one half of the unit cell cannot point towards one another. This seems a reasonable assumption because if they point towards one another, then internuclear distance becomes about 1.9Å. Secondly it is necessary to take a positive in order to get agreement with the observed values of α_b. The sign of b is still undetermined. If, however, we choose b to be negative (according to the conventional orientation of the axes) the hydrogen assumes a much more likely position in the unit cell than for b positive. The resulting orientation of the OH group in the first layer of the Bravais cell is shown in Figure 9.

Our result may now be compared with that given by Tsuboi. Corresponding to the values we find of 15° and 58° respectively for the angles HOB and BOA (Fig. 9), Tsuboi obtained values of 20° and 51°. He discarded these values as improbable on symmetry considerations and replaced them with the figures 16.5° and 60° attributing the difference to "the vibration of the H atoms about their equilibrium positions". It is clear from our work that this last assumption is unnecessary. We can only conclude that Tsuboi's measurements of the absorption coefficients are in error for some unknown reason.

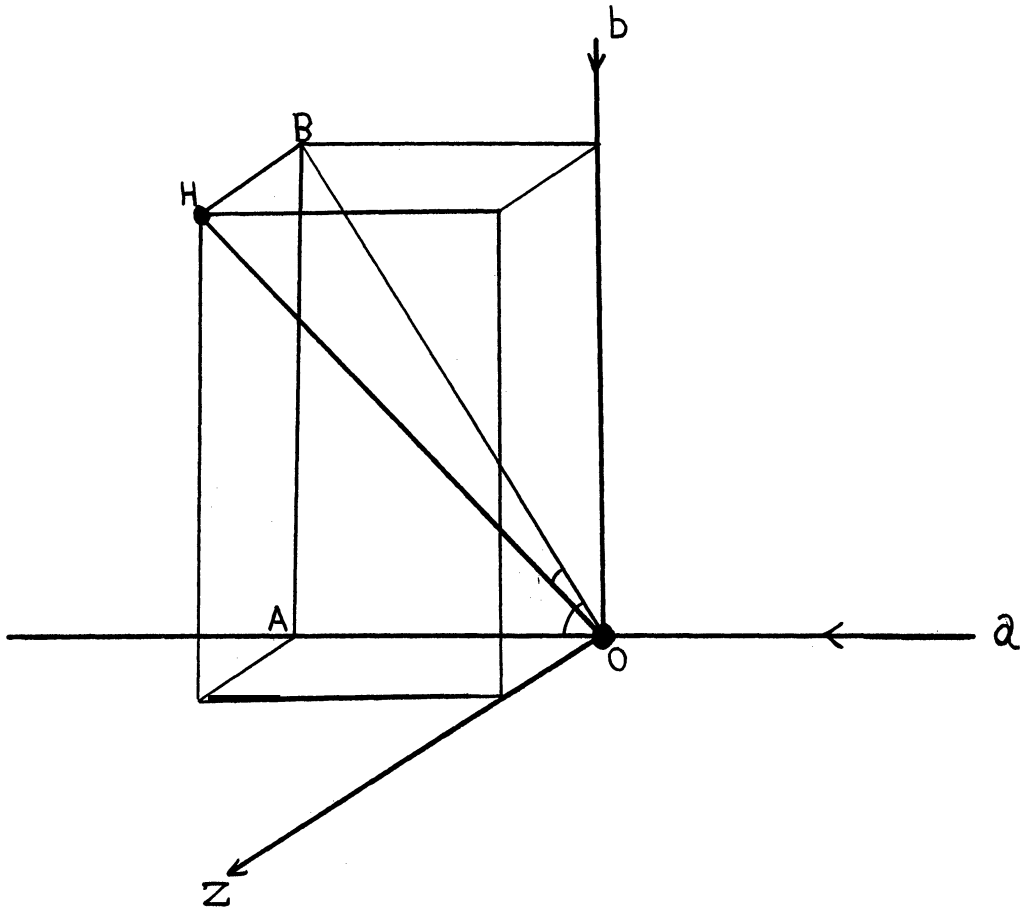

Fig. 9 The Orientation of OH group (No. 1 in Fig. 5) in Muscovite. $\angle HOB = 15°$, $\angle BOA = 58°$

The work of Vergnoux, Theron and Pouzol[2] enabled them to determine only the angle BOA (Fig. 9) for which they obtained a value of 59°. Our value for this angle is 58°. Thus our results agree with those obtained by an entirely independent method viz. birefringence measurements.

Symmetry Properties and Selection Rules for OH Vibrations in Biotite

The space group of biotite does not appear to have been determined by X-ray methods. We assumed at first that it was the same as muscovite (i.e. C_{2h}^6) but this would not account for the fact that biotite shows two well resolved OH stretching frequencies near 3μ where muscovite has only one. If, however, the Bravais cell for biotite is twice as large as that for muscovite, then this doubling becomes understandable. We were led in this way to the conclusion that the space group for biotite must be C_{2h}^4 instead of C_{2h}^6, but initially we assumed that this distinction only applied when the positions of the hydrogen atoms were taken into account. Subsequent examination of a model of biotite in which only the positions of the atoms heavier than hydrogen are considered has shown that biotite can belong to the C_{2h}^4 space group. The proof will be outlined, although it is hard to follow without a spatial model.

The necessary and sufficient conditions for a lattice to have a C_{2h}^6 space group can be described in the following way[11]. Take the origin of coordinates at a center of symmetry (i) and the x, y and z axes parallel to the crystallographic axes a,

b and c respectively (Fig. 5). For any arbitrary position (x, y, z) the following coordinates must be equivalent:

(1) $x \pm a/2$, $y \pm b/2$, z.

(2) $\bar{x}$, $\bar{y}$, $\bar{z}$.

(3) $\bar{x}$, y, $c/2 - z$.

(4) x, $\bar{y}$, $c/2 + z$.

This means that if (x, y, z) represent the coordinates of any of the atoms in the unit cell, then an equivalent atom will be found at the position given by these four transformations. It may readily be verified from a model that these conditions are fulfilled by all the atoms in muscovite. However, condition (1) cannot be fulfilled by the Fe and Mg atoms in biotite. Since the necessary and sufficient conditions for a C_{2h}^4 space group are just (2), (3) and (4), (which correspond respectively to the symmetry elements i, C_2 and σ_h^g), and can be fulfilled by all of the atoms in biotite, we conclude that the space group for biotite should be C_{2h}^4 instead of C_{2h}^6.

It should be remarked that the partial replacement (i.e. one quarter) of the Si atoms by Al atoms in the SiO_4 tetrahedra means that strictly speaking the conditions for C_{2h}^6 and C_{2h}^4 space groups are exactly fulfilled by none of the micas. However, the conditions are fulfilled by the O atoms of the OH^- groups and the selection rules are essentially determined by this fact.

The Bravais cell for the C_{2h}^4 space group is exactly twice as large as that for the C_{2h}^6 space group. It coincides with

the conventional crystallographic unit cell of Fig. 5 and thus contains 8 OH^- groups. The resulting 48 fundamental modes of vibration fall into 4 symmetry species as shown in Table III. Thus there are now 4 OH^- stretching modes active in infrared absorption. The physical character of these four modes is illustrated in Figs. 10 and 11 together with the resulting changes of electric moment. The pair of modes shown in Fig. 10 may be expected to have the same frequency value for the same reason that the two active modes in muscovite had the same numerical value, i.e. negligible interaction across the plane of the K^+ ions. The same is true for the other pair of Fig. 11.

TABLE III

C_{2h}^4	E	C_2	i	σ_h^g	n	D	T	IR	R
A_g	1	1	1	1	2	4	6	f	p
A_u	1	1	-1	-1	2	4	6	p	f
B_g	1	-1	1	-1	2	4	6	f	p
B_u	1	-1	-1	1	2	4	6	p	f

In order to construct Figs. 10 and 11 it was necessary to assume a direction for one of the 4 OH^- groups which are inside the Bravais cell for muscovite and another direction for one of the 4 OH^- groups which are outside of this cell. The orientations of all of the 8 OH^- groups in the Bravais cell of the C_{2h}^4 space group are then fixed by symmetry.

Using the same notation as for muscovite, we may now write down expressions for the absorption coefficients of the two absorption bands as functions of a_1, b_1, z_1, a_2, b_2, z_2 (the

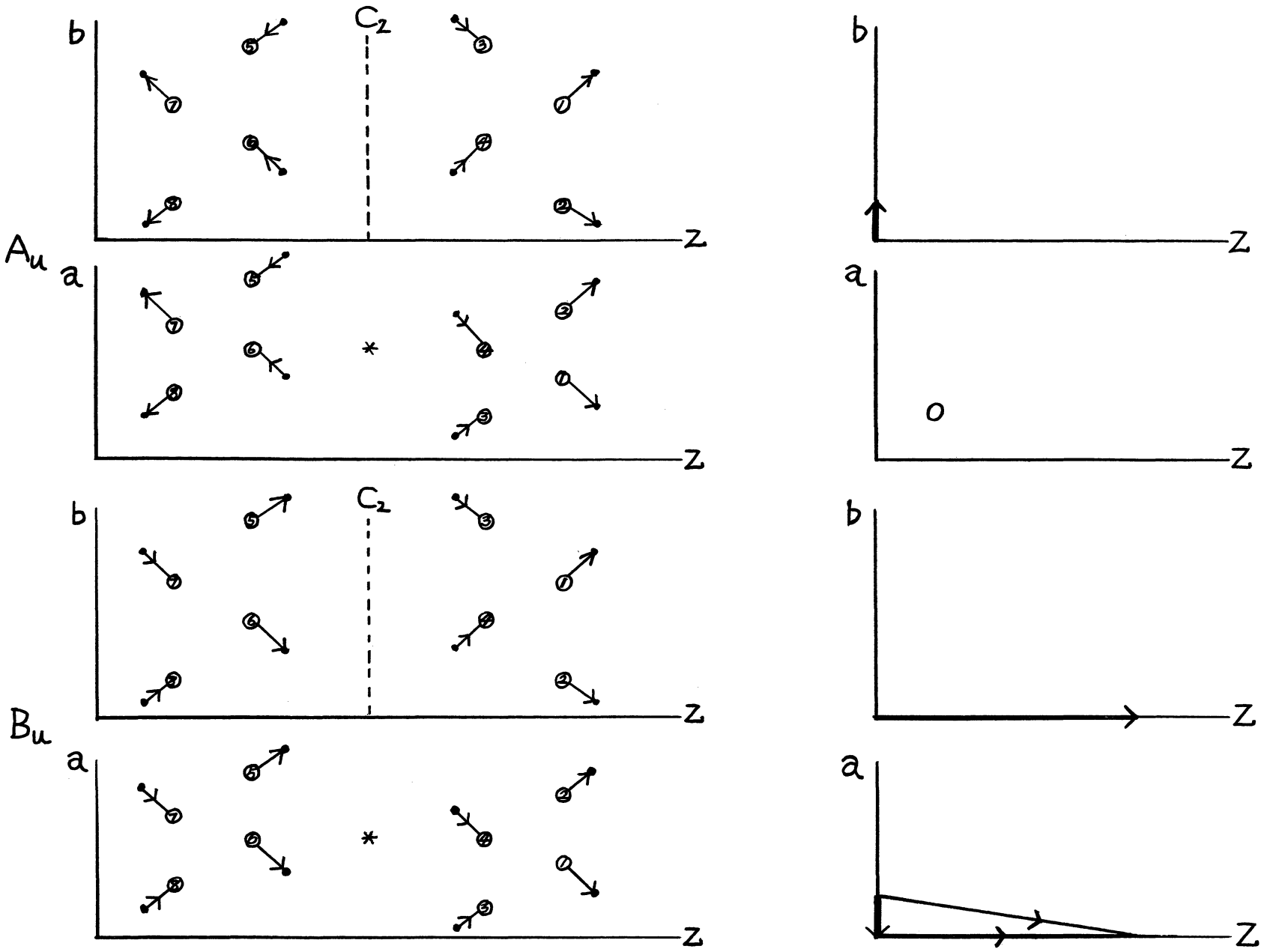

FIGURE 10. MODES of OH Stretching Vibrations of Biotite and the Corresponding Electric Moment Change (2.72μ band)

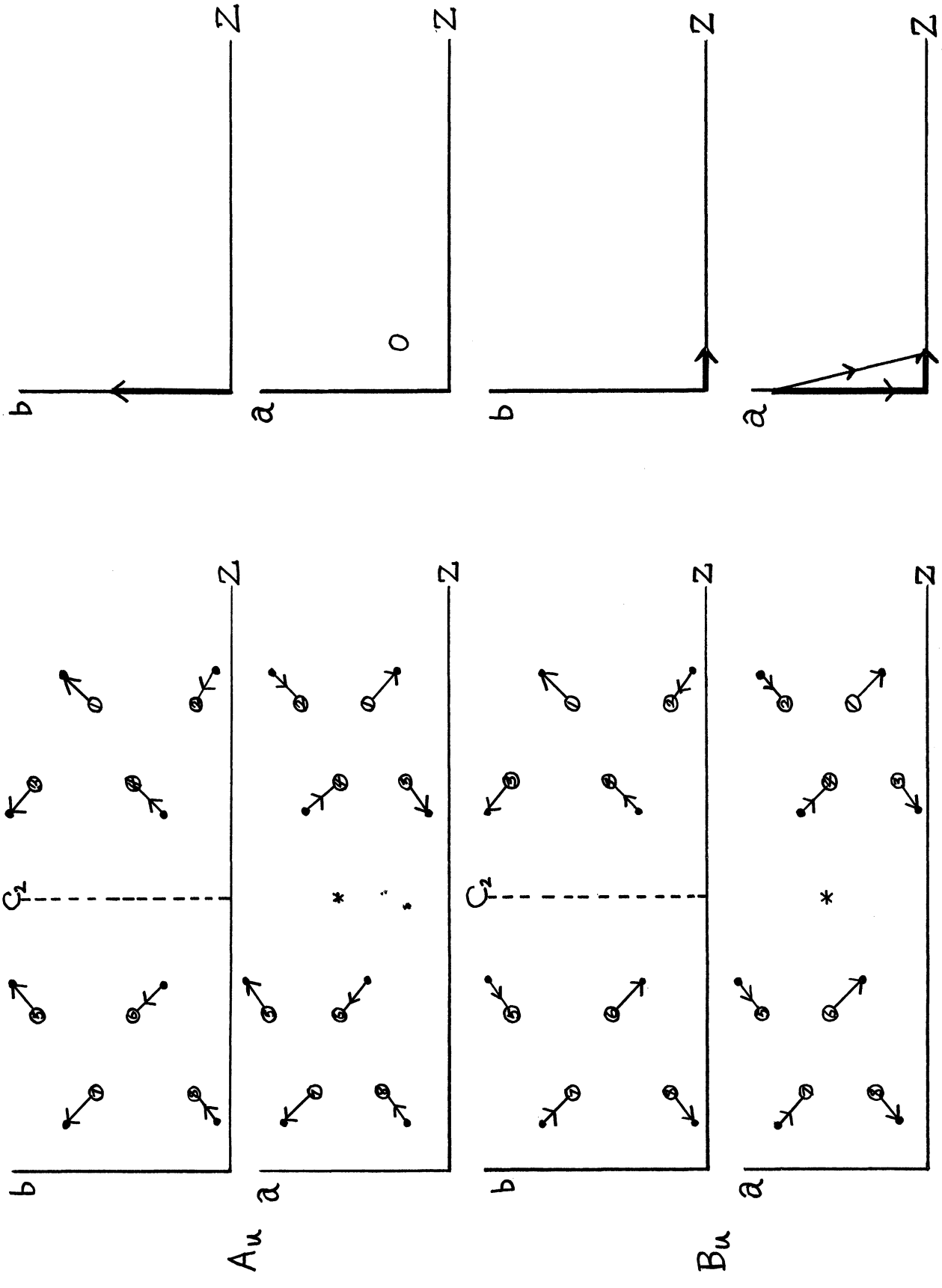

FIGURE 11. MODES of OH Stretching Vibrations of Biotite and the Corresponding Electric Moment Change (2.83μ band)

respective displacement coordinates of any one of the inner 4 hydrogen atoms and any one of the outer 4 hydrogen atoms) and r. Thus we obtain:

For Modes of Vibration of Figure 10 (2.72μ absorption band)

$$\alpha_b \propto \left[4(a_1 - a_2)\cos r + 4(z_1 + z_2)\sin r\right]^2, \quad \alpha_b^\circ \propto \left[4(b_1 - b_2)\right]^2$$

$$\alpha_a \propto \left[4(b_1 - b_2)\cos r\right]^2 + \left[4(z_1 + z_2)\sin r\right]^2, \text{ and } \alpha_a^\circ \propto \left[4(a_1 - a_2)\right]^2$$

For Modes of Vibration of Figure 11 (2.83μ absorption band)

$$\alpha_b \propto \left[4(a_1 + a_2)\cos r + 4(z_1 + z_2)\sin r\right]^2, \quad \alpha_b^\circ \propto \left[4(b_1 + b_2)\right]^2$$

$$\alpha_a \propto \left[4(b_1 + b_2)\cos r\right]^2 + \left[4(z_1 + z_2)\sin r\right]^2, \text{ and } \alpha_a^\circ \propto \left[4(a_1 + a_2)\right]^2$$

The orientations of the crystal which should be considered for these vibrations are illustrated in Fig. 12 and 13.

It should be noted that the orientations of the OH^- groups here are assumed in an arbitrary way. The true values (relative) of a_1, b_1, z_1, etc. have to be determined by experimental results. We may now discuss the experimental data on biotite.

Experimental Results on Biotite

The same techniques were used here as for muscovite and the results are summarized in Table IV and V. The crystal section was much thicker (225μ) than for muscovite. A typical series of spectra is illustrated in Fig. 14, while Fig. 15 illustrates the variation in the absorption coefficients of each band as the crystal is tilted about either the a or the b axis. It will be noticed in Fig. 14 that the high frequency band (2.72μ) increases greatly in intensity for tilting about either the a or the b axis. Thus the change of moment for this

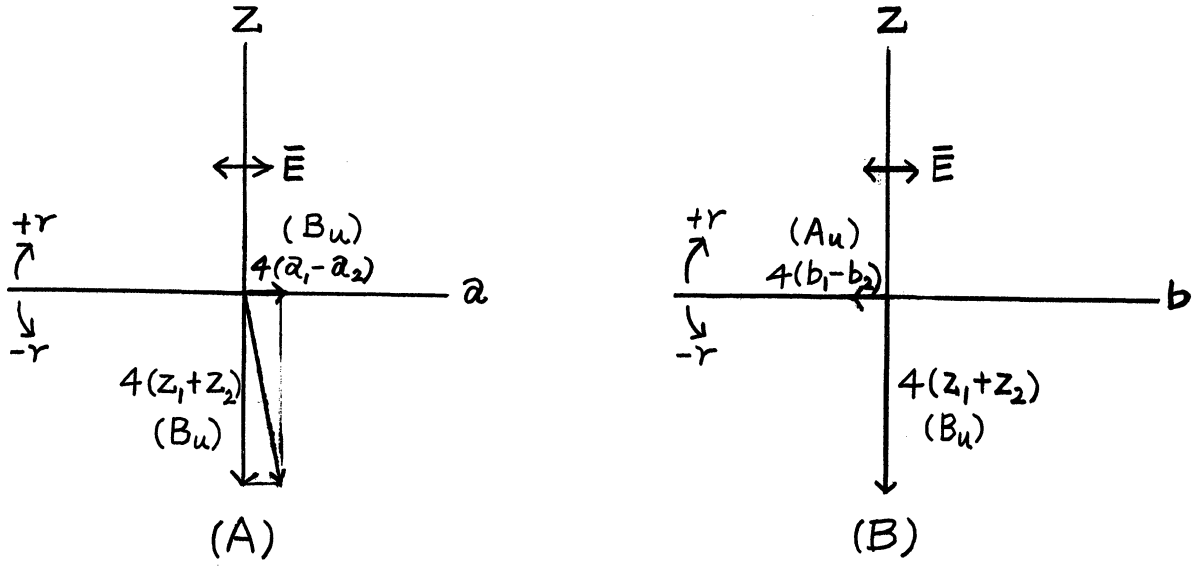

Fig 12. Orientations of Biotite and Electric Moment Change of OH Stretching Vibrations (2.72μ band). (A) and (B) similar to Fig. 7.

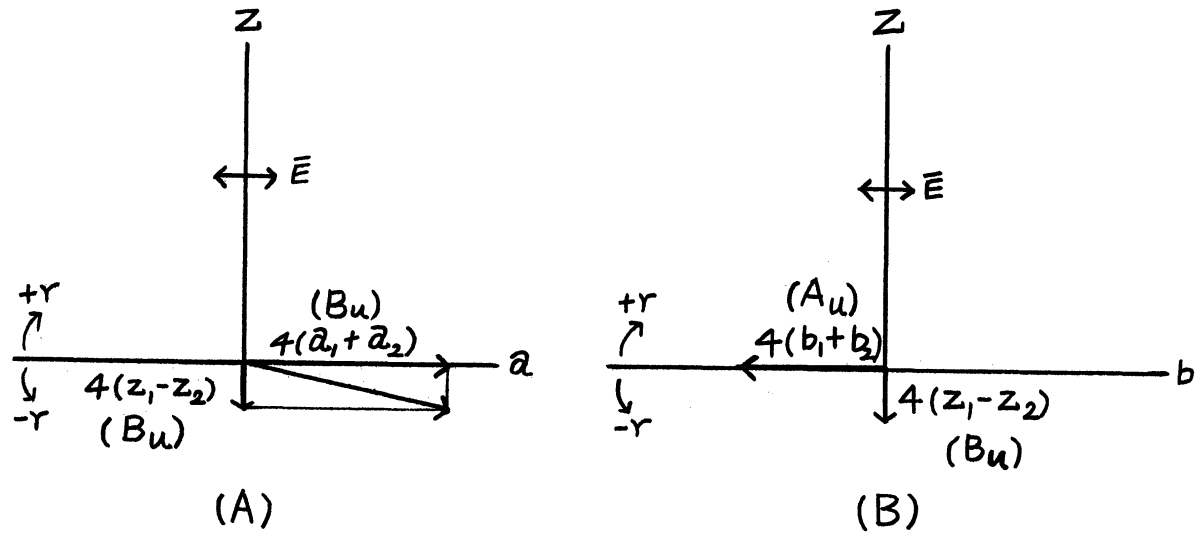

Fig. 13. Orientation of Biotite and Electric Moment Change of OH Stretching Vibrations (2.83μ band). (A) and (B) similar to Fig. 7.

TABLE IV Absorption Coefficients of 2.72μ Band

		Tilted about b axis		Tilted about a axis	
		$\vec{E} \perp b$		$\vec{E} \perp a$	
i	r	α_b (Obs.)	α_b (Cal.)	α_a (Obs.)	α_a (Cal.)
-40°	-23°55'	1.053	1.280	1.061	1.280
-30°	-18°23'	.750	.774	.772	.774
-20°	-12°28'	.391	.362	.439	.362
-10°	- 6°17'	.079	.093	.109	.093
0	0	0	0	0	0
+10°	+ 6°17'	.115	.093	.103	.093
+20°	+12°28'	.442	.362	.443	.362
+30°	+18°23'	.779	.774	.795	.774
+40°	+23°55'	1.097	1.280	1.109	1.280

TABLE V Absorption Coefficients of 2.83μ Band

		$\vec{E} \perp b$		$\vec{E} \perp a$	
i	r	α_b (Obs.)	α_b (Cal.)	α_a (Obs.)	α_a (Cal.)
-40°	-23°55'	.541	.490	.437	.406
-30°	-18°23'	.564	.528	.457	.437
-20°	-12°28'	.582	.559	.470	.463
-10°	- 6°17'	.583	.580	.485	.480
0	0	.587	.587	.486	.486
+10°	+ 6°17'	.562	.580	.485	.480
+20°	+12°28'	.535	.559	.479	.463
+30°	+18°23'	.517	.528	.458	.437
+40°	+23°55'	.475	.490	.424	.406

Tilted about b axis Tilted about a axis

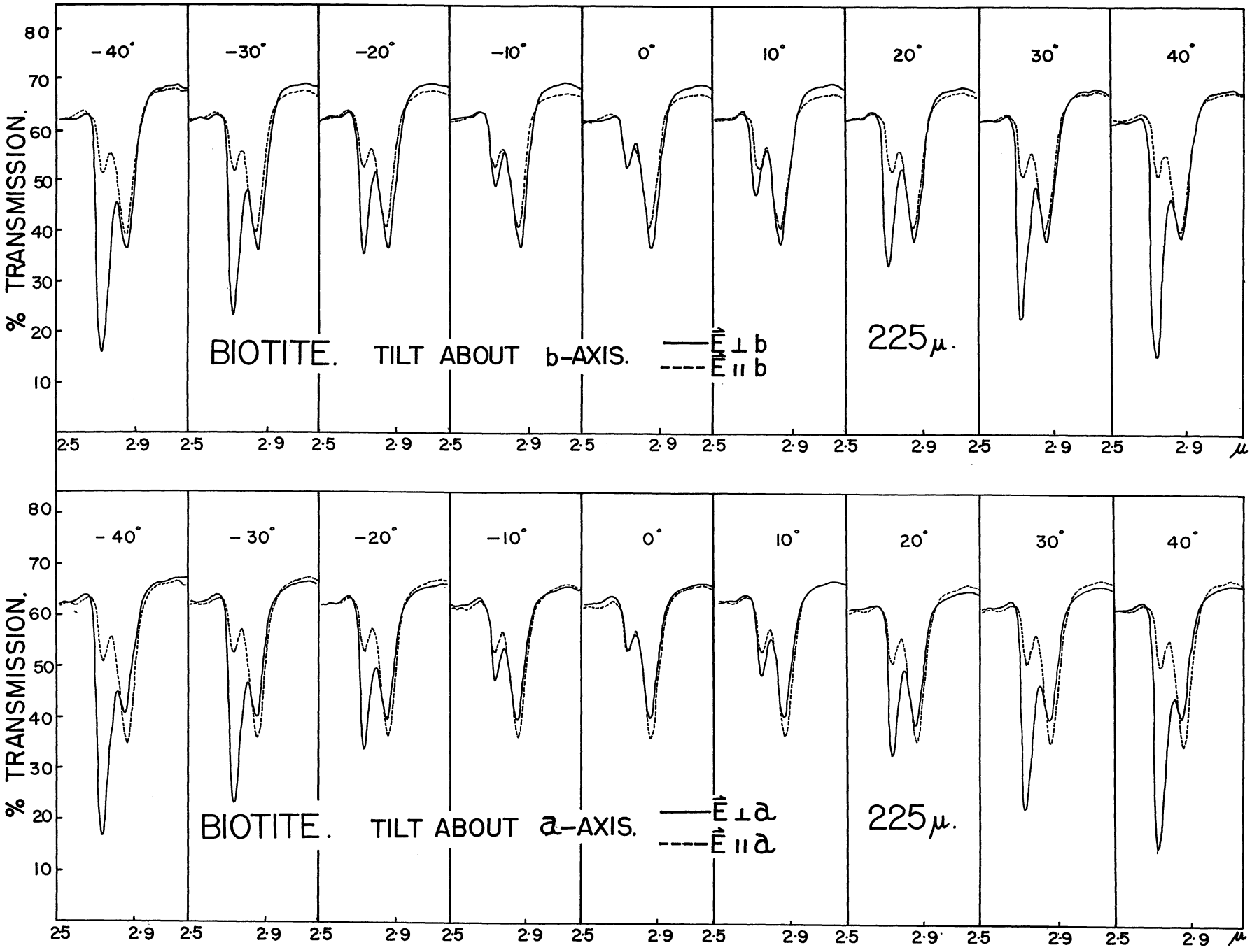

Fig. 14. Spectra of Biotite

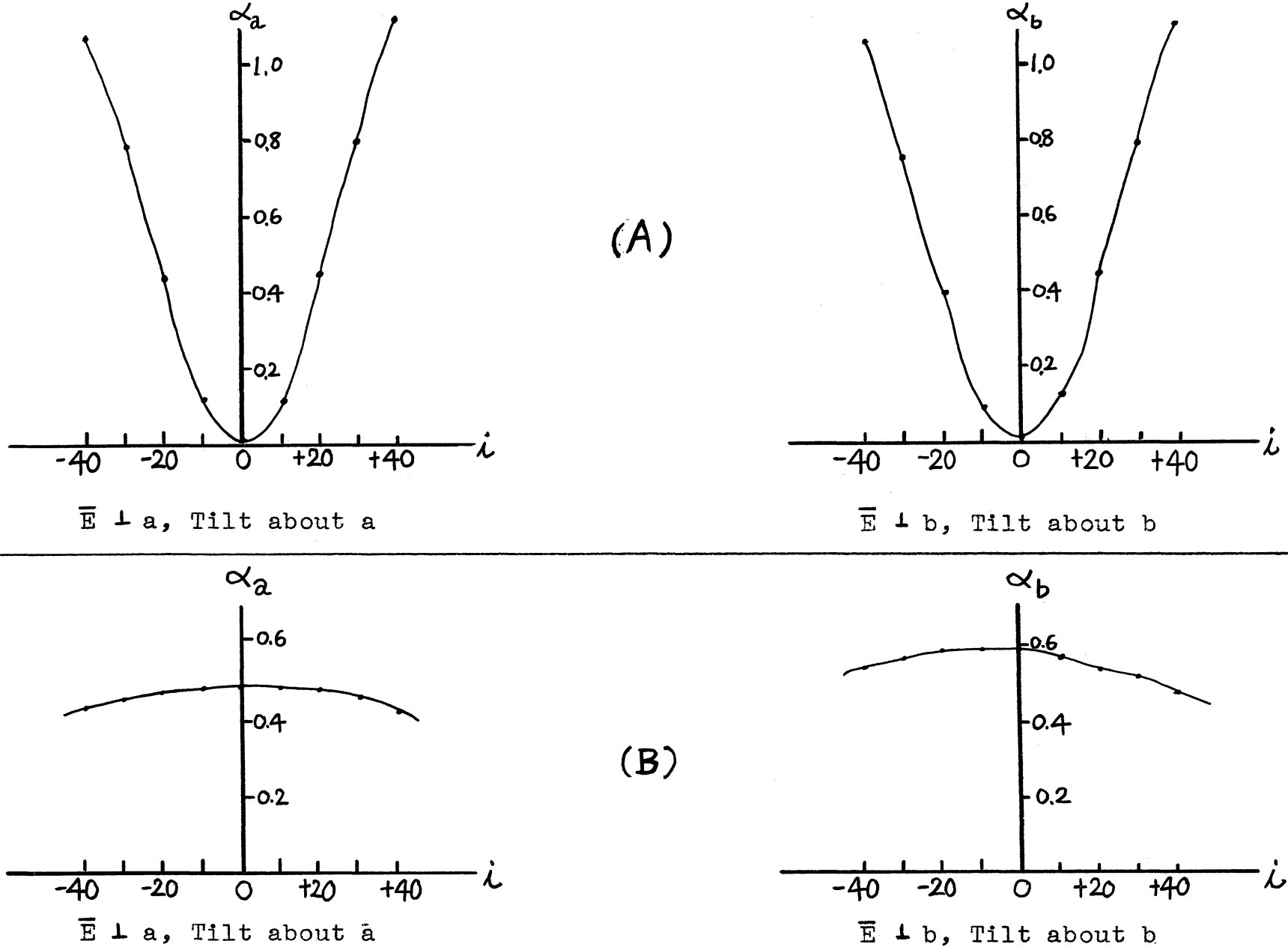

$\bar{E} \perp$ a, Tilt about a

$\bar{E} \perp$ b, Tilt about b

$\bar{E} \perp$ a, Tilt about ā

$\bar{E} \perp$ b, Tilt about b

FIGURE 15. Variation of Absorption Coefficients (A) 2.72μ band, (B) 2.83μ band.

mode of vibration must be almost entirely along z (or c) axis. This corresponds to the behavior predicted for the mode of vibration of Fig. 10 if a_1 and b_1 are respectively nearly equal to a_2 and b_2. We therefore assign the 2.72μ band to Fig. 10 mode. Similarly the 2.83μ band is assigned to Fig. 11 mode. If there were no absorption at 2.72μ for normal incidence, the change of moment should be exactly along the z axis. Investigation of the behavior of this band at low and high temperature made it appear that this residual absorption for normal incidence was due to other causes (c.f. Quarterly Report I of September 1954) and in this report we shall ignore this absorption. That means we assume $a_1 = a_2$ and $b_1 = b_2$, and we shall call them just a and b. In Table IV we shall assume it is zero as a first approximation.

According to Fig. 13(A), if the difference between z_1 and z_2 is large, we should observe an asymmetric variation in the absorption coefficient of the 2.83μ band as the crystal is tilted about the b axis to the positive (+r) or negative (-r) side of its original position. The variation of α_b in Table V shows very little asymmetry indicating that z_1 and z_2 are nearly equal. Therefore we shall also assume $z_1 = z_2 = z$ as a first approximation.

In computing α, the refractive index was assumed to be 1.585. We may now compute a, b and z from the experimental data as follows:-

Using the data from the 2.83μ band with normal incidence, we have

$$(8a)^2 = (.587) \quad \text{and} \quad (8b)^2 = (.486)$$

giving $\quad 8a = \pm .766 \quad \text{and} \quad 8b = \pm .697$

Using next the data from the 2.72μ band with i $= \pm 30°$,

$r = \pm 18°23'$, for tilt about b or a and $\overline{E}$ perpendicular to b or a we get

$$(8z \sin r)^2 = (8z \sin 18°23')^2 = 0.774 \text{ (average value)}$$

giving $\quad 8z = \pm 2.79.$

If now these values of a, b and z are substituted in the above expressions for α_a and α_b for each band, we obtain predicted values for α_a and α_b for all other angles. These values are given in the fourth and sixth columns of Table IV and V.

The resulting orientation of the OH group in the first layer of the unit cell is shown in Fig. 16. The sign of z can be reasonably assumed as positive because if the hydrogen atoms point towards one another the internuclear H-H distance will be less than 1Å. The signs of a and b cannot be determined by computation. These are under investigation now, and a full discussion will be given in a subsequent report.

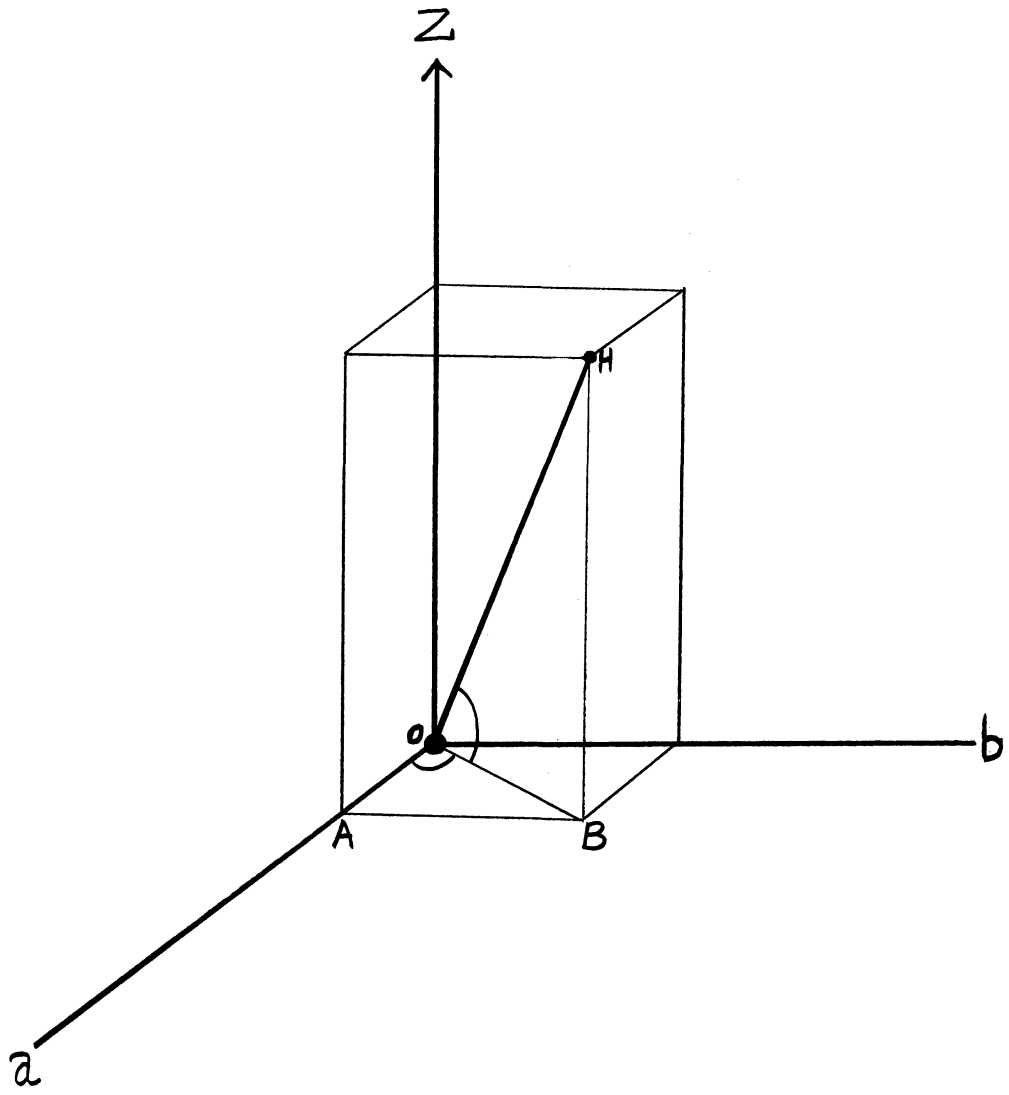

Fig. 16. The Orientation of OH Group (No. 1 in Fig. 5) in Biotite. $\angle HOB = 70°$, $\angle BOA = 42°$.

REFERENCES

1 M. Tsuboi, Bull. Chem. Soc., Japan 23, 83 (1950)

2 A. M. Vergnoux, Comptes Rendus. 238, 467 (1954)

3 C. H. Mauguin, Bull. Soc. Franc. Min. 51, 285 (1928)

4 L. Pauling, "The Nature of the Chemical Band", Cornell University Press, (1942)

5 W. W. Jackson and J. West, Zeit. f. Krist 76, 211 (1930) and 85, 160 (1933)

6 G. Nagelschmidt, Zeit. f. Krist, 97, 514 (1937)

7 C. W. Brindley, "X-ray Identification and Crystal Structure of Clay Minerals", Mineralogical Society of London, (1951)

8 W. L. Bragg, "Atomic Structure of Minerals", Cornell University Press, (1937)

9 S. Bhagavantam and T. Venkatarayudu, "Theory of Groups and its Application to Physical Problems", Andhra University, Waltair, India, (1951)

10 T. R. P. Gibb Jr., "Optical Methods of Chemical Analysis", McGraw-Hill Book Company, Inc., (1942)

11 International Tables for X-ray Crystallography, Volume I, Kynoch Press, Bermingham, England, (1952)

V. MAJOR CONCLUSIONS

A. Barium Titanate

The experimental work done on barium titanate does not support the theory of Jaynes. At present, it also does not support that of Megaw, but observations at longer wavelengths are required to verify this tentative conclusion.

B. Diamond

The work on diamond gives strong support to the idea that Type I diamonds are imperfect but does not yet establish the source of imperfection. There are probably several sources of imperfection, foreign atoms or carbon atoms in anomalous states being most strongly indicated.

C. Brucite

Our investigations on brucite lead to the conclusion that either the unit cell is much larger than that determined by X-ray methods which have not placed the hydrogen atoms correctly or some new effect has been found in the infra-red spectra of crystals which cannot be explained in current theories of the vibration spectra of crystals.

D. Micas

The work on the micas has shown that the orientation of the OH groups in muscovite and biotite are very different. There is a strong indication that biotite belongs to the C_{2h}^4 space group in contrast to muscovite which belongs to the C_{2h}^6 space group. The orientations of the OH groups in muscovite and biotite have

not yet been absolutely determined, but it has been possible to reduce the choice of these orientations to a very limited number of possibilities.

VI. FUTURE PROGRAM

A. Barium Titanate

Work will continue on the differences between the infra-red spectra of the various forms of barium titanate and also the spectrum of strontium titanate. Once real differences have been established, it is hoped that these will throw light on the origin of ferroelectricity in barium titanate.

B. Diamond

An attempt will be made to determine the nature of chemical impurities in various diamonds (Type I and Type II) by means of spectrographic (emission) analysis.

C. Brucite

If time and personnel are available, an attempt will be made to resolve the disagreement found here between X-ray and infra-red methods of analysis of the structure of brucite.

D. Micas

Work will continue on the determination of the absolute orientation of the OH groups in muscovite and biotite. The over-all interpretation of the spectra of all micas will also be studied.

VII. PERSONNEL

The following people have been engaged in the work described in this report.

Prof. G. B. B. M. Sutherland, Principal Investigator

Dr. R. T. Mara (November 1951 - August 1953)

Dr. W. G. Simeral (June 1951 - June 1953 Part Time)

Dr. C. Y. Pan Liang (March 1953 - May 1954 Half Time)

Dr. T. Venkatarayudu (February - May 1954)

Dr. S. Krimm (May 15 - August 15, 1951 Part Time)

Mr. H. J. V. Tyrell (September 1 - October 31, 1951)

Mr. G. Allen (October - December 1953 Part Time)

Mr. A. Dockrill (May 1951 - May 1954 Part Time as Laboratory Technician)

VIII. Appendix I

(This is a more complete version of the note published in Jour. of Chem. Physics 22:1269 (1954)

SELECTION RULES FOR SOME COMBINATION AND OVERTONE LINES IN DIAMOND

by

T. Venkatarayudu, M.A., Ph.D., F.A.Sc.

Structure of Diamond:- Diamond may be regarded as having been made up of two interpenetrating cubic face-centered simple structure of carbon atoms. Each atom of one structure is at the center of the tetrahedron formed by its four nearest neighbours of the other structure. The positions of the carbon atoms in the crystal are usually described with reference to the

crystallographic axes, which are the edges of a cube. Accordingly, the co-ordinates of the eight atoms in the unit cube are given by (0,0,0), (1/2,1/2,1/2), (1/2,0,1/2), (0,1/2,1/2), (1/4,1/4,1/4), (3/4,3/4,1/4), (3/4,1/4,3/4), (1/4,3/4,3/4). The above description is convenient for enumerating the symmetry elements of the crystal. But for a study of the frequency spectrum of diamond, it is advantageous to describe the co-ordinates of the atoms in the Bravais cell. The Bravais cell, in this case, is the parellelopiped formed by the edges 12, 13 and 14 and contains only two non-equivalent atoms (1 and 5 in the figure). (Two atoms are said to be equivalent, if one of them can be obtained from the other by means of a lattice translation.

Factor Group Analysis:- It is well known that all modes of oscillation, other than those in which equivalent atoms have identical motion, are forbidden in their fundamentals both in Raman effect and in the Infra-red absorption. Normal modes in which equivalent atoms have identical motion may be studied by considering the crystallographic point group of the crystal. The effect of a translational operation of symmetry on such modes is the same as that of identity. The symmetry operations of the point group O_h^7, the appropriate character table and the selection rules for the fundamental modes etc. are tabulated below with the usual notation. Symmetry modes coming under A_{1g}, E_g and F_{2u} are Infra-red active. We thus see that diamond has only one normal mode of oscillation which is active in its fundamental in Raman effect and forbidden in the Infra-Red

absorption.

O_h^7	E	$8C_3$	$3C_2$	6	$6S_4$	i	$8S_6$	3	$6C_2$	$6C_4$	k_i
A_{1g}	1	1	1	1	1	1	1	1	1	1	o Raman Active
A_{2g}	1	1	1	-1	-1	1	1	1	-1	-1	o
E_g	2	-1	2	o	o	2	-1	2	o	o	o Raman Active
F_{1g}	3	o	-1	-1	1	3	o	-1	-1	1	o
F_{2g}	3	o	-1	1	-1	3	o	-1	1	-1	1 Raman Active
A_{1u}	1	1	1	1	1	-1	-1	-1	-1	-1	o
A_{2u}	1	1	1	-1	-1	-1	-1	-1	1	1	o
E_u	2	-1	2	o	o	-2	1	-2	o	o	o
F_{1u}	3	o	-1	-1	1	-3	o	1	1	-1	o
F_{2u}	3	o	-1	1	-1	-3	o	1	-1	1	1 Translation(M)
U_R	2	2	2	2	2	o	o	o	o	o	
	6	o	-6	12	-12	o	o	o	o	o	

Finite Space Group Analysis:- A detailed study of the Finite Space Group Analysis is under investigation. In the following discussion, we restrict ourselves to the case where the motions of atoms separated by twice the primitive translations are identical. The repeating unit cell is then formed by taking eight times the Bravais cell. This cell contains 16 non-equivalent atoms. (Two atoms are now called equivalent if one can be obtained from the other by twice a primitive translation.)

In the figure is shown a portion of the diamond structure. The dark circles denote atoms belonging to one simple structure whereas the white circles denote the atoms belonging to the other.

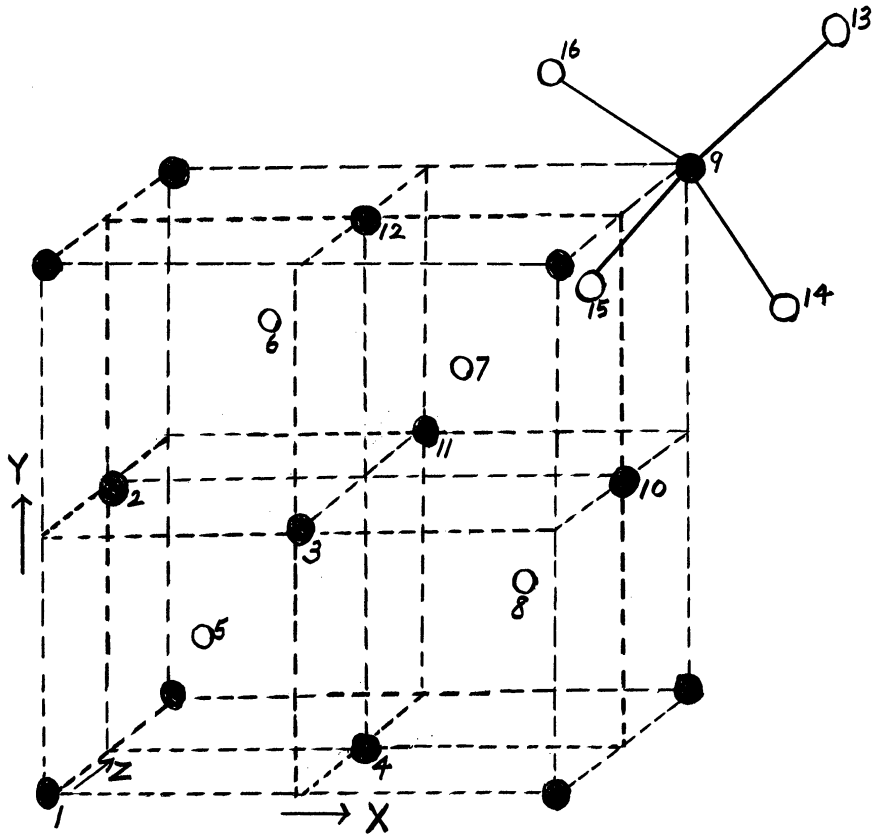

FIGURE

The Bravais cell is a rhombohedron formed by the primitive translations T_1, T_2, T_3 respectively obtained by joining the atoms 1,2; 1,3; 1,4;. This rhombohedron contains only two non-equivalent atoms which are numbered 1 and 5. The unit cell which we now choose is the rhombohedron formed by the primitive translations which are twice 1,2; 1,3; and 1,4;. This rhombohedron contains 16 non-equivalent atoms which are numbered 1 to 16 in the figure. The co-ordinates of the atoms referred to cubic axes are given below.

1,2,3,4: 0,0,0; 0,1/2,1/2; 1/2,1/2,0; 1/2,0,1/2.

5,6,7,8: 1/4,1/4,1/4; 1/4,3/4,3/4; 3/4,3/4,1/4; 3/4,1/4,3/4.

9,10,11,12: 1,1,1; 1,1/2,1/2; 1/2,1/2,1; 1/2,1,1/2.

13,14,15,16: 5/4,5/4,5/4; 5/4,3/4,3/4; 3/4,3/4,5/4; 3/4,5/4,3/4.

The group of symmetry elements now is of order 384 and they are obtained by combining the eight translations with the 48 elements of symmetry which form the crystallographic point group O_h^7. The elements of this group fall into 20 conjugate classes and the appropriate character table, symmetry modes coming under each type are given below. The representations designated

$$A_1,\ A_2,\ A_3,\ A_4,\ E_1,\ E_2,\ F_1,\ F_2,\ F_3,\ F_4$$

correspond to the factor group representations

$$A_{1g},\ A_{2g},\ A_{1u},\ A_{2u},\ E_g,\ E_u,\ F_{1g},\ F_{2g},\ F_{1u},\ F_{2u}$$

respectively. A_1 E_1 F_2 may be called the activity representations for Raman effect and the representation F_4 may similarly be called the activity representation for the infra-red. We further give below the reduction of the product representations

and also the reduction of the symmetric square representations from which we can directly read the selection rules for the simple combination lines and the first overtones.

																					K_i
A_1	1	1	1	1	1	1	1	1	1	1	1	1	1	1	1	1	1	1	1	1	0
A_2	1	1	-1	-1	-1	1	1	-1	-1	-1	-1	1	-1	-1	-1	1	1	1	-1	1	0
A_3	1	1	1	1	1	-1	-1	-1	-1	-1	-1	1	1	1	1	-1	-1	-1	-1	1	0
A_4	1	1	1	-1	-1	-1	-1	-1	1	1	1	1	-1	1	-1	1	-1	-1	1	1	0
E_1	2	-1	2	0	0	2	-1	2	0	0	0	2	0	-1	0	2	2	-1	0	2	0
E_2	2	-1	2	0	0	-2	1	-2	0	0	0	2	0	-1	0	2	-2	1	0	2	0
F_1	3	0	-1	-1	1	3	0	-1	-1	1	-1	3	-1	0	-1	-1	3	0	-1	3	0
F_2	3	0	-1	1	-1	3	0	-1	1	-1	1	3	1	0	1	-1	3	0	1	3	1
F_3	3	0	-1	-1	+1	-3	0	+1	1	-1	1	3	-1	0	-1	-1	-3	0	1	3	0
F_4	3	0	-1	1	-1	-3	0	1	-1	1	-1	3	1	0	1	-1	-3	0	-1	3	1
H_1	6	0	2	2	0	0	0	0	0	0	0	-2	-2	0	2	-2	0	0	0	6	1
H_2	6	0	-2	0	0	0	0	0	2	0	-2	-2	0	0	0	2	0	0	-2	6	1
H_3	6	0	2	-2	0	0	0	0	0	0	0	-2	2	0	-2	-2	0	0	0	6	0
H_4	6	0	-2	0	0	0	0	0	-2	0	2	-2	0	0	0	2	0	0	2	6	1
L_1	4	1	0	2	0	2	1	0	0	0	-2	0	0	-1	-2	0	-2	-1	2	-4	1
L_2	4	1	0	-2	0	2	1	0	0	0	2	0	0	-1	2	0	-2	-1	-2	-4	0
L_3	4	1	0	2	0	-2	-1	0	0	0	2	0	0	-1	-2	0	2	1	-2	-4	1
L_4	4	1	0	-2	0	-2	-1	0	0	0	-2	0	0	-1	2	0	2	1	2	-4	0
M_1	8	-1	0	0	0	4	-1	0	0	0	0	0	0	1	0	0	-4	1	0	-8	1
M_2	8	-1	0	0	0	-4	1	0	0	0	0	0	0	1	0	0	4	-1	0	-8	1
U_R	16	4	4	8	2	0	0	0	0	0	0	0	0	0	0	0	0	0	0	0	0
x	48	0	-48	96	-96	0	0	0	0	0	0	0	0	0	0	0	0	0	0	0	0

Simple Combinations:

$E_1 \times L_1 = M_1$	$E_2 \times L_1 = M_2$
$E_1 \times L_2 = M_1$	$E_2 \times L_2 = M_2$
$E_1 \times L_3 = M_2$	$E_2 \times L_3 = M_1$
$E_1 \times L_4 = M_2$	$E_2 \times L_4 = M_1$
$E_1 \times M_1 = L_1 + L_2 + M_1$	$E_2 \times M_1 = L_3 + L_4 + M_2$
$E_1 \times M_2 = L_3 + L_4 + M_2$	$E_2 \times M_2 = L_1 + L_2 + M_1$
$F_1 \times F_1 = A_1 + E_1 + F_1 + F_2$	
$F_1 \times F_2 = A_2 + E_1 + F_1 + F_2$	$F_2 \times F_2 = A_1 + E_1 + F_1 + F_2$
$F_1 \times F_3 = A_3 + E_2 + F_3 + F_4$	$F_2 \times F_3 = A_4 + E_2 + F_3 + F_4$
$F_1 \times F_4 = A_4 + E_2 + F_3 + F_4$	$F_2 \times F_4 = A_3 + E_2 + F_3 + F_4$ (I.R.)
$F_1 \times H_1 = H_2 + H_3 + H_4$	$F_2 \times H_1 = H_1 + H_2 + H_4$
$F_1 \times H_2 = H_1 + H_3 + H_4$	$F_2 \times H_2 = H_1 + H_2 + H_3$
$F_1 \times H_3 = H_1 + H_2 + H_4$	$F_2 \times H_3 = H_2 + H_3 + H_4$
$F_1 \times H_4 = H_1 + H_2 + H_3$	$F_2 \times H_4 = H_1 + H_3 + H_4$
$F_1 \times L_1 = L_2 + M_1$	$F_2 \times L_1 = L_1 + M_1$
$F_1 \times L_2 = L_1 + M_1$	$F_2 \times L_2 = L_2 + M_1$
$F_1 \times L_3 = L_4 + M_2$	$F_2 \times L_3 = L_3 + M_2$
$F_1 \times L_4 = L_3 + M_2$	$F_2 \times L_4 = L_4 + M_2$
$F_1 \times M_1 = L_1 + L_2 + 2\,M_1$	$F_2 \times M_1 = L_1 + L_2 + 2\,M_1$
$F_1 \times M_2 = L_3 + L_4 + 2\,M_2$	$F_2 \times M_2 = L_3 + L_4 + 2\,M_2$
$F_3 \times F_3 = A_1 + E_1 + F_1 + F_2$	
$F_3 \times F_4 = A_2 + E_1 + F_1 + F_2$	$F_4 \times F_4 = A_1 + E_1 + F_1 + F_2$
$F_3 \times H_1 = H_2 + H_3 + H_4$	$F_4 \times H_1 = H_2 + H_3 + H_4$
$F_3 \times H_2 = H_1 + H_2 + H_3$	$F_4 \times H_2 = H_1 + H_3 + H_4$
$F_3 \times H_3 = H_1 + H_2 + H_4$	$F_4 \times H_3 = H_2 + H_3 + H_4$
$F_3 \times H_4 = H_1 + H_3 + H_4$	$F_4 \times H_4 = H_1 + H_3 + H_4$

$F_3 \times L_1 = L_4 + M_2$ $\quad$ $F_4 \times L_1 = L_3 + M_2$

$F_3 \times L_2 = L_3 + M_2$ $\quad$ $F_4 \times L_2 = L_4 + M_2$

$F_3 \times L_3 = L_2 + M_1$ $\quad$ $F_4 \times L_3 = L_1 + M_1$

$F_3 \times L_4 = L_1 + M_1$ $\quad$ $F_4 \times L_4 = L_2 + M_1$

$F_3 \times M_1 = L_3 + L_4 + 2\,M_2$ $\quad$ $F_4 \times M_1 = L_3 + L_4 + 2\,M_2$

$F_3 \times M_2 = L_1 + L_2 + 2\,M_1$ $\quad$ $F_4 \times M_2 = L_1 + L_2 + 2\,M_1$

$A_1 \times A_1 = A_1$			
$A_1 \times A_2 = A_2$	$A_2 \times A_2 = A_1$		
$A_1 \times A_3 = A_3$	$A_2 \times A_3 = A_4$	$A_3 \times A_3 = A_1$	
$A_1 \times A_4 = A_4$	$A_2 \times A_4 = A_3$	$A_2 \times A_4 = A_2$	$A_4 \times A_4 = A_1$
$A_1 \times E_1 = E_1$	$A_2 \times E_1 = E_1$	$A_3 \times E_1 = E_2$	$A_4 \times E_1 = E_2$
$A_1 \times E_2 = E_2$	$A_2 \times E_2 = E_2$	$A_3 \times E_2 = E_1$	$A_4 \times E_2 = E_1$
$A_1 \times F_1 = F_1$	$A_2 \times F_1 = F_2$	$A_3 \times F_1 = F_3$	$A_4 \times F_1 = F_4$
$A_1 \times F_2 = F_2$	$A_2 \times F_2 = F_1$	$A_3 \times F_2 = F_4$	$A_4 \times F_2 = F_3$
$A_1 \times F_3 = F_3$	$A_2 \times F_3 = F_4$	$A_3 \times F_3 = F_1$	$A_4 \times F_3 = F_2$
$A_1 \times F_4 = F_4$	$A_2 \times F_4 = F_3$	$A_3 \times F_4 = F_2$	$A_4 \times F_4 = F_1$
$A_1 \times H_1 = H_1$	$A_2 \times H_1 = H_3$	$A_3 \times H_1 = H_1$	$A_4 \times H_1 = H_3$
$A_1 \times H_2 = H_2$	$A_2 \times H_2 = H_4$	$A_3 \times H_2 = H_4$	$A_4 \times H_2 = H_2$
$A_1 \times H_3 = H_3$	$A_2 \times H_2 = H_1$	$A_3 \times H_3 = H_3$	$A_4 \times H_3 = H_1$
$A_1 \times H_4 = H_4$	$A_2 \times H_4 = H_2$	$A_3 \times H_4 = H_2$	$A_4 \times H_4 = H_4$
$A_1 \times L_1 = L_1$	$A_2 \times L_1 = L_2$	$A_3 \times L_1 = L_3$	$A_4 \times L_1 = L_4$
$A_1 \times L_2 = L_2$	$A_2 \times L_2 = L_1$	$A_3 \times L_2 = L_4$	$A_4 \times L_2 = L_3$
$A_1 \times L_3 = L_3$	$A_2 \times L_3 = L_4$	$A_3 \times L_3 = L_1$	$A_4 \times L_3 = L_2$
$A_1 \times L_4 = L_4$	$A_2 \times L_4 = L_3$	$A_3 \times L_4 = L_2$	$A_4 \times L_4 = L_1$
$A_1 \times M_1 = M_1$	$A_2 \times M_1 = M_1$	$A_3 \times M_1 = M_2$	$A_4 \times M_1 = M_2$
$A_1 \times M_2 = M_2$	$A_2 \times M_2 = M_2$	$A_3 \times M_2 = M_1$	$A_4 \times M_2 = M_1$

$E_1 \times E_1 = A_1 + A_2 + E_1$

$E_1 \times E_2 = A_3 + A_4 + E_2$

$E_1 \times F_1 = F_1 + F_2$

$E_1 \times F_2 = F_1 + F_2$

$E_1 \times F_3 = F_3 + F_4$

$E_1 \times F_4 = F_3 + F_4$

$E_1 \times H_1 = H_1 + H_3$

$E_1 \times H_2 = H_2 + H_4$

$E_1 \times H_3 = H_1 + H_3$

$E_1 \times H_4 = H_2 + H_4$

$E_2 \times E_2 = A_1 + A_2 + E_2$

$E_2 \times F_1 = F_3 + F_4$

$E_2 \times F_2 = F_3 + F_4$

$E_2 \times F_3 = F_1 + F_2$

$E_2 \times F_4 = F_1 + F_2$

$E_2 \times H_1 = H_1 + H_3$

$E_2 \times H_2 = H_2 + H_4$

$E_2 \times H_3 = H_1 + H_3$

$E_2 \times H_4 = H_2 + H_4$

$H_1 \times H_1 = A_1 + A_3 + E_1 + E_2 + F_2 + F_4 + H_1 + H_2 + H_3 + H_4$

$H_1 \times H_2 = F_1 + F_2 + F_3 + F_4 + H_1 + H_2 + H_3 + H_4$ (Both)

$H_1 \times H_3 = A_2 + A_4 + E_1 + E_2 + F_1 + F_3 + H_1 + H_2 + H_3 + H_4$

$H_1 \times H_4 = F_1 + F_2 + F_3 + F_4 + H_1 + H_2 + H_3 + H_4$ (Both)

$H_1 \times L_1 = L_1 + L_3 + M_1 + M_2$

$H_1 \times L_2 = L_2 + L_4 + M_1 + M_2$

$H_1 \times L_3 = L_1 + L_3 + M_1 + M_2$

$H_1 \times L_4 = L_2 + L_4 + M_1 + M_2$

$H_1 \times M_1 = L_1 + L_2 + L_3 + L_4 + 2\,M_1 + 2\,M_2$

$H_1 \times M_2 = L_1 + L_2 + L_3 + L_4 + 2\,M_1 + 2\,M_2$

$H_2 \times H_2 = A_1 + A_4 + E_1 + E_2 + F_2 + F_3 + H_1 + H_2 + H_3 + H_4$

$H_2 \times H_3 = F_1 + F_2 + F_3 + F_4 + H_1 + H_2 + H_3 + H_4$

$H_2 \times H_4 = A_2 + A_3 + E_1 + E_2 + F_1 + F_4 + H_1 + H_2 + H_3 + H_4$ (Raman)

$H_2 \times L_1 = L_2 + L_3 + M_1 + M_2$

$H_2 \times L_2 = L_1 + L_4 + M_1 + M_2$

$H_2 \times L_3 = L_1 + L_4 + M_1 + M_2$

$H_2 \times L_4 = L_2 + L_3 + M_1 + M_2$

$H_2 \times M_1 = L_1 + L_2 + L_3 + L_4 + 2\,(M_1 + M_2)$

$H_2 \times M_2 = L_1 + L_2 + L_3 + L_4 + 2\,(M_1 + M_2)$

$H_3 \times H_3 = A_1 + A_3 + E_1 + E_2 + F_2 + F_4 + H_1 + H_2 + H_3 + H_4$

$H_3 \times H_4 = F_1 + F_2 + F_3 + F_4 + H_1 + H_2 + H_3 + H_4$

$H_3 \times L_1 = L_2 + L_4 + M_1 + M_2$

$H_3 \times L_2 = L_1 + L_3 + M_1 + M_2$

$H_3 \times L_3 = L_2 + L_4 + M_1 + M_2$

$H_3 \times L_4 = L_1 + L_3 + M_1 + M_2$

$H_3 \times M_1 = L_1 + L_2 + L_3 + L_4 + 2\,(M_1 + M_2)$

$H_3 \times M_2 = L_1 + L_2 + L_3 + L_4 + 2\,(M_1 + M_2)$

$H_4 \times H_4 = A_1 + A_4 + E_1 + E_2 + F_2 + F_3 + H_1 + H_2 + H_3 + H_4$

$H_4 \times L_1 = L_1 + L_4 + M_1 + M_2$

$H_4 \times L_2 = L_2 + L_3 + M_1 + M_2$

$H_4 \times L_3 = L_2 + L_3 + M_1 + M_2$

$H_4 \times L_4 = L_1 + L_4 + M_1 + M_2$

$H_4 \times M_1 = L_1 + L_2 + L_3 + L_4 + 2\,(M_1 + M_2)$

$H_4 \times M_2 = L_1 + L_2 + L_3 + L_4 + 2\,(M_1 + M_2)$

$L_1 \times L_1 = A_1 + F_2 + H_1 + H_4$

$L_1 \times L_2 = A_2 + F_1 + H_2 + H_3$ $\qquad L_2 \times L_2 = A_1 + F_2 + H_1 + H_4$

$L_1 \times L_3 = A_3 + F_4 + H_1 + H_2$ (I.R) $\qquad L_2 \times L_3 = A_4 + F_3 + H_3 + H_4$

$L_1 \times L_4 = A_4 + F_3 + H_3 + H_4$ $\qquad L_2 \times L_4 = A_3 + F_4 + H_1 + H_2$

$L_1 \times M_1 = E_1 + F_1 + F_2 + H_1 + H_2 + H_3 + H_4$ (Raman)

$L_1 \times M_2 = E_2 + F_3 + F_4 + H_1 + H_2 + H_3 + H_4$ (I.R.)

$L_2 \times M_1 = E_1 + F_1 + F_2 + H_1 + H_2 + H_3 + H_4$

$L_2 \times M_2 = E_2 + F_3 + F_4 + H_1 + H_2 + H_3 + H_4$

$L_3 \times L_3 = A_1 + F_1 + H_1 + H_4$

$L_3 \times L_4 = A_2 + F_1 + H_2 + H_3$ $\qquad$ $L_4 \times L_4 = A_1 + F_2 + H_1 + H_4$

$L_3 \times M_1 = E_2 + F_3 + F_4 + H_1 + H_2 + H_3 + H_4$ (I.R.)

$L_3 \times M_2 = E_1 + F_1 + F_2 + H_1 + H_2 + H_3 + H_4$ (Raman)

$L_4 \times M_1 = E_2 + F_3 + F_4 + H_1 + H_2 + H_3 + H_4$

$L_4 \times M_2 = E_1 + F_1 + F_2 + H_1 + H_2 + H_3 + H_4$

$M_1 \times M_1 = A_1 + A_2 + E_1 + 2\,(F_1 + F_2 + H_1 + H_2 + H_3 + H_4)$

$M_1 \times M_2 = A_3 + A_4 + E_2 + 2\,(F_3 + F_4 + H_1 + H_2 + H_3 + H_4)$ (I.R.)

$M_2 \times M_2 = A_1 + A_2 + E_1 + 2\,(F_1 + F_2 + H_1 + H_2 + H_3 + H_4)$

<u>FIRST Overtones</u>:

$(A_1)_2 = (A)_1$

$(A_2)_2 = A_1$

$(A_3)_2 = A_1$

$(A_4)_2 = A_1$

$(E_1)_2 = A_1 + E_1$

$(E_2)_2 = A_1 + E_1$

$(F_1)_2 = (F_2)_2 = (F_3)_2 = (F_4)_2 = A_1 + E_1 + F_2$

$(H_1)_2 = (H_2)_2 = (H_3)_2 = (H_4)_2 = A_1 + A_4 + E_1 + E_2 + F_2 + H_1 + H_4$

$(L_1)_2 = (L_2)_2 = (L_3)_2 = (L_4)_2 = A_1 + F_2 + H_1 + H_4$

$(M_1)_2 = (M_2)_2 = A_1 + E_1 + F_1 + 2\,F_2 + 2\,H_1 + H_3 + H_4$

It follows from the previous analysis that the combination lines

$$H_1 \times H_2 \qquad \text{and} \qquad H_1 \times H_4$$

are active both in Raman Effect and Infra-red absorption.

The author's sincere thanks are due to Professors D. M. Dennison and G. B. B. M. Sutherland for their kind interest in this work.

Reprinted from JOURNAL OF THE OPTICAL SOCIETY OF AMERICA, Vol. 43, No. 11, 1100–1102, November, 1953
Printed in U. S. A.

The Infrared Spectrum of Brucite [$Mg(OH)_2$]*

R. T. MARA† AND G. B. B. M. SUTHERLAND
University of Michigan, Ann Arbor, Michigan
(Received August 17, 1953)

The infrared spectrum of single crystals of brucite [$Mg(OH)_2$] has been examined under high resolving power between 2 and 3μ. It contains at least 16 bands most of which are shown to be OH stretching frequencies and which exhibit a variety of polarization properties. It follows that the unit cell of brucite must be much larger than had been previously assumed and that the positions of the hydrogen atoms have been incorrectly assigned from x-ray data.

INTRODUCTION

IN the course of a study of the infrared spectra of a number of crystalline materials (including mica) it recently became important to investigate in detail the spectrum of a crystal of known structure containing hydroxyl groups or ions. Furthermore, it was desirable to have a crystal in which the OH groups (or ions) were all oriented in the same direction and were not hydrogen bonded. According to the x-ray work of Bernal and Megaw,[1] magnesium hydroxide [$Mg(OH)_2$] in the form of brucite crystals fulfills both criteria. In order to see whether the latter was fulfilled, our first action was of course to see what Coblentz[2] had recorded on the spectra of crystals containing hydroxyl groups. In a research dealing with the differences between the infrared spectra of water of crystallization and water of constitution, Coblentz noted that the infrared spectrum of brucite appeared to be anomalous. All the other compounds that he had studied, containing OH groups and ions, showed a characteristic band at 2.9μ to 3.0μ, but brucite was peculiar in that it exhibited a band with a strong maximum at 2.5μ with indications of weaker maxima near 2.7μ and 3.0μ. This "anomaly" was very satisfactory from our point of view since it indicated that any hydrogen bonding effect in brucite must be much weaker than it is in alcohols, for instance, where the free OH band is shifted (as in water) from 2.75μ to 3.0μ.

In this paper we present the preliminary results of our work on the spectrum of brucite, using polarized radiation and high resolving power on single crystals in various orientations. This spectrum has turned out to be extremely complex and of great significance, especially in the relation of infrared to x-ray methods of investigating molecular structure in the crystalline state.

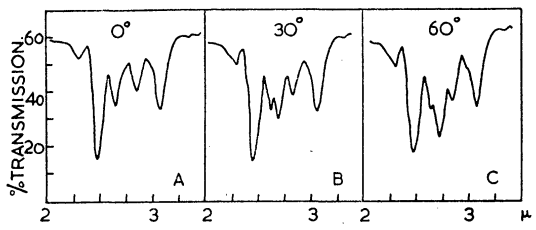

FIG. 1. Infrared spectrum of brucite oriented with c axis parallel to the incident beam and at angles of 30° and 60°.

EXPERIMENTAL RESULTS

The most striking new feature revealed by our reexamination of the infrared spectrum of brucite is the discovery of a highly complex structure in the band observed by Coblentz near 2.5μ. The spectrum of a cleaved section of brucite with the incident beam parallel to the c axis (i.e., normal to the cleavage plane) is given in Fig. 1(A). This spectrum was obtained with a Perkin-Elmer Model 21 double-beam spectrophotometer equipped with a rock salt prism. While the early work showed absorption in this interval with maximum absorption near 2.5μ [the approximate position of the most intense band in Fig. 1(A)], none of these details were available to Coblentz, who chose only a few points between 2μ and 3μ for his point-by-point plot. The strongest absorption band is found near 2.48μ, and weaker ones are observed at roughly 2.30μ, 2.65μ, 2.83μ, and 3.07μ. It is to be noted that no band is observed near 2.75μ, which is the approximate location of a "free" OH vibration band in many compounds. However, the four principal absorption maxima are located in a roughly symmetrical pattern about this wavelength. The remainder of the spectrum out to 15μ for this crystal orientation is generally in agreement with that reported by Coblentz and will not be discussed further in this paper.

If the crystal is inclined so that the c axis is no longer parallel to the incident beam, then a new band appears near 2.73μ, and its intensity increases with increasing angle between the c axis and the incident beam [Fig. 1(B) and 1(C)]. Polarization spectra of a crystal tilted in this way indicate that the 2.73-μ band is present in the spectrum only when the incident electric vector has a component parallel to the c axis of the crystal. Identical results are obtained when the crystal is rotated about any axis that lies perpendicular to the c axis.

All the bands that appear on the spectrum when the incident beam is parallel to the c axis are also observed

* Supported by the U. S. Army Signal Corps.
† Present address, Department of Physics, Gettysburg College, Gettysburg, Pennsylvania.
[1] J. D. Bernal and H. D. Megaw, Proc. Roy. Soc. (London) A151, 384 (1935).
[2] W. W. Coblentz, *Investigations of Infrared Studies* (Carnegie Institution of Washington, Washington, D. C., 1905–1908).

when the beam is normal to the c axis, and in addition the 2.73-μ band and its overtone are present. The polarization effects for this orientation are very marked. The polarized spectra from 2μ to 3.25μ are shown in Fig. 2. The bands at 2.30μ, 2.73μ (and probably also that at 2.83μ) exhibit maximum intensities when the electric vector is parallel to the c axis. The absorption near 2.48μ changes contour for the two polarization directions, and it appears to have a diminished intensity when the electric vector is parallel to the c axis. The 2.65μ and 3.07μ display their maximum intensities for the electric vector perpendicular to the c axis.

Since a rock salt prism does not have large dispersion below 8μ, a LiF prism was used to scan the 2μ- to 3.2-μ region. Portions of the spectra with this higher resolution are given in Fig. 3. These spectra are for orientations of the crystal with the c axis parallel and perpendicular to the direction of the incident beam. It is immediately seen that the absorption maxima in Figs.

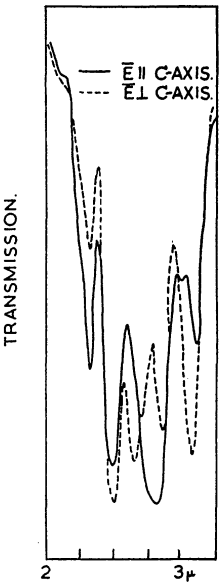

FIG. 2. Polarized infrared spectra of brucite with incident electric vector E parallel and perpendicular to the c axis.

1 and 2 are composed of several bands. The absorption complex near 2.5μ is especially interesting, since it consists of four individual absorption maxima, only one of which is common to both orientations. Also, the frequency shift in the band near 3.07μ is of interest. While the high resolution spectrum of the absorption near 2.73μ is not reproduced here, we can report that it is composed of at least two bands at 2.71μ and 2.74μ, each of which exhibits its maximum intensity when the c axis is oriented perpendicular to the incident beam. In all, sixteen bands have been observed between 2μ and 3.1μ in the spectrum of brucite, and all of these are listed in Table I. Those listed in the first column are observed in the spectrum when the incident electric vector is perpendicular to the c axis, and those in the second column appear when the electric vector is parallel to the c axis. The polarization properties are also given, where $P(N)$ indicates maximum absorption for the incident electric vector E parallel (normal) to

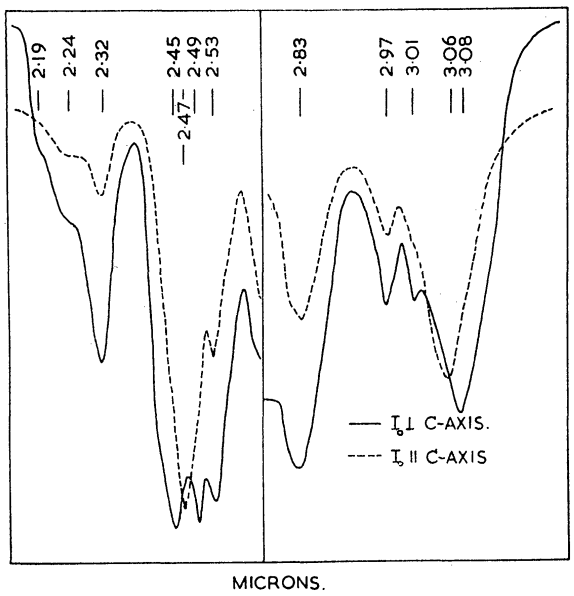

FIG. 3. Portions of infrared spectra of brucite for crystal c axis oriented parallel and perpendicular to the incident beam.

the c axis. Those values that are in brackets represent bands which may be present for a particular orientation but which may be obscured by neighboring absorptions.

Between the time of Coblentz's and our observations, other infrared studies of brucite have also been made by Plyler,[3] Yeou Ta,[4] Duval and Lecomte,[5] and Louisfert,[6] But none of this work revealed anything more than Coblentz had in the region of the OH stretching fundamental.

DISCUSSION

If the structure of brucite had been as postulated by Bernal and Megaw, then the OH stretching frequency should have given rise to a single sharp absorption line near 2.75μ. This follows from their contention that

TABLE I. Infrared absorption bands of brucite.

$E \perp c$ axis	$E \parallel c$ axis
2.06μ	2.06μ
2.19	2.19 P
2.24	2.24
2.32	2.32 P
(2.45)	2.45 P
2.47	(2.47) N
(2.49)	2.49 P
2.53	2.53 P
2.64	(2.64) N
2.71	2.71 P
	2.74 P
2.83	2.83 P(?)
2.97	2.97
3.01	3.01
3.06	3.06 N
	3.08 P

[3] E. K. Plyler, Phys. Rev. **28**, 284 (1926).
[4] M. Yeou Ta, Compt. rend. **211**, 467 (1940).
[5] C. Duval and J. Lecomte, bull. Soc. chim. **8**, 713 (1941); Bull. soc. franç. minéral. **66**, 284 (1943).
[6] J. Louisfert, J. phys. radium **8**, 21 (1947).

the unit cell contains only two OH ions and from the rules set up by Bhagavantam and Venkatarayuda,[7] Halford,[8] and Hornig[9] for the infrared spectra of crystals. That is the OH normal modes of a unit cell would consist of simply the in-phase and out-of-phase OH vibrations. One of these gives a zero net dipole moment change and hence is infrared inactive, leaving only one infrared active frequency associated with the hydroxyl vibrations. This band should show perfect polarization, with the change of moment parallel to the c axis.

Such a band is indeed observed by us, but there are in addition at least 15 other bands in the immediate neighborhood exhibiting a variety of polarization properties. It might be argued that these represent combination vibrations with low lattice frequencies involving the Mg^{++} ions. However, this cannot be so, for we have examined the spectrum of $Mg(OD)_2$ and the complex pattern of bands is moved by a constant factor (nearly $\sqrt{2}$) to longer wavelengths. It follows that most of the bands observed between 2μ and 3.1μ are true OH stretching frequencies, although a small number of them could conceivably be combinations of OH stretching fundamentals with OH deformation lattice modes. This means that the unit cell for brucite must be very large indeed, containing at least as many OH^- ions as there are OH stretching fundamentals observed. Furthermore, from the polarization properties of these bands it is certain that the positions of the hydrogen atoms have been incorrectly assigned from the x-ray data. A full treatment of the problem together with a discussion of interesting features of the brucite spectrum at other wavelengths is reserved for a later paper. Our purpose here was twofold: (a) To show that one of the pebbles picked by Coblentz on the infrared beach as of some interest is indeed a very fascinating one when examined by modern instruments; (b) to demonstrate the much greater sensitivity of the infrared method (as compared to the x-ray method) in deciding about the positions of hydrogen atoms in crystals.

[7] S. Bhagavantam and T. Venkatarayuda, Proc. Indian Acad. Sci. **A9**, 224 (1939).
[8] R. S. Halford, J. Chem. Soc. **14**, 8 (1946).
[9] D. F. Hornig, J. Chem. Soc. **16**, 1063 (1948).